

**NACA**

**RESEARCH MEMORANDUM**

APR 18 1947

CANOPY LOADS INVESTIGATION FOR THE F6F-3 AIRPLANE

By

Bennie W. Cocke, Jr., and K. R. Czarnecki

Langley Memorial Aeronautical Laboratory  
Langley Field, Va.

**NATIONAL ADVISORY COMMITTEE  
FOR AERONAUTICS**

WASHINGTON  
April 14, 1947

**NACA LIBRARY**  
LANGLEY MEMORIAL AERONAUTICAL  
LABORATORY

NATIONAL ADVISORY COMMITTEE FOR AERONAUTICS

RESEARCH MEMORANDUM

CANOPY LOADS INVESTIGATION FOR THE F6F-3 AIRPLANE

By Bennie W. Cocks, Jr., and K. R. Czarnecki

SUMMARY

In conjunction with a general investigation of the aerodynamic forces on cockpit enclosures, surface static pressures have been measured over both the outer and inner surfaces of the cockpit canopies on the Grumman F6F-3, Curtiss SB2C-4E, and Grumman F8F-1 airplanes in the Langley full-scale tunnel. This paper presents a preliminary analysis of data obtained for the F6F-3 airplane. Plots are presented that show the distribution of pressure at four lateral stations through the canopy for a range of conditions selected to determine the effects of varying canopy position, yaw, lift coefficient, and power. The results indicate that the net aerodynamic loads on the canopy are greatest when the airplane is operating at high speed with the canopy closed. At all attitudes investigated the effect of opening the canopy is to reduce the internal-external pressure differential, therefore reducing the exploding forces. Asymmetrical loading is shown for numerous conditions due to propeller operation and airplane yaw but is most extreme at positive yaw attitudes with propeller operating.

INTRODUCTION

The occurrence of canopy failures on Navy airplanes in flight has indicated that present load requirements used in the design of canopies and their components may not be adequate. As the current load requirements are based on wind-tunnel pressure distributions obtained over a range of pitch and yaw attitudes with the canopy closed and do not include accurate measurement of internal pressure or the effects of canopy opening, it is desirable that these factors be investigated and the critical load conditions more accurately defined.

As a result, the Bureau of Aeronautics, Navy Department, has requested the Langley Laboratory of the National Advisory Committee for Aeronautics to conduct a general investigation to determine the critical load requirements by means of external and internal pressure

measurements on airplanes employing three representative types of canopies. The three types of canopies selected for the tests were the conventional single-sliding enclosure, conventional front and rear-sliding enclosures, and the bubble-type enclosures which are typified by the installation on the Grumman F6F-3, Curtiss SB2C-4E, and Grumman F8F-1 airplanes, respectively.

As the first phase of this investigation, tests have been made in the Langley full-scale tunnel to determine external and internal pressure distributions on the three types of canopies for an extensive range of simulated flight conditions with canopy position varied from closed to full open. This paper presents the results obtained with the conventional single-sliding canopy on the F6F-3 airplane.

### AIRPLANE

The F6F-3 airplane is a single-place low-wing fighter airplane having a wing span of 42 feet 10 inches, a wing area of 334 square feet, and a normal gross weight of 11,441 pounds. The airplane is powered by a Pratt & Whitney R-2800 engine having an engine propeller gear ratio of 2 to 1. The engine has a military power rating of 2000 horsepower at 2700 rpm at sea level. The engine drives a 13-foot 1-inch-diameter 3-blade Hamilton Standard propeller. A three-view drawing giving the principal dimensions of the airplane is shown in figure 1. Figure 2 shows the airplane mounted in the full-scale tunnel.

The cockpit enclosure on this airplane consists of a single conventional rearward sliding canopy equipped with emergency release mechanism. The canopy has no curvature in the side panels and has approximately constant cross section from front to rear. The windshield fairing ahead of the canopy is rounded and intersects the fuselage at an angle of approximately  $45^\circ$ . At the rear the canopy fairings tangent to the fuselage afterbody. Figure 3 shows the general canopy arrangement.

### METHODS AND TESTS

Surface static pressures over the cockpit canopy were measured by means of flush-type static orifices installed in nine longitudinal rows along the canopy (fig. 4). Internal canopy pressures were measured by means of four  $\frac{1}{8}$ -inch static pressure tubes installed

on the inner surface of the canopy at locations indicated in figure 4.

The external and internal pressures were measured with propeller removed and with propeller operating and with the canopy set in

four positions: namely, closed, 3 inches open,  $\frac{1}{2}$  open, and full open.

The tests were made with the airplane set at angles of attack corresponding to lift coefficients of 0.20, 0.52, 0.91, and 1.23 which were determined from force tests with propeller removed (fig. 5). The tests with propeller removed indicated that the canopy pressures were only slightly affected by large changes in lift coefficient. It was believed, therefore, that any changes in lift coefficient due to propeller operation would have little effect on the canopy pressures. Consequently, the values of angle of attack used during the tests with propeller removed were duplicated for the tests with propeller operating. The specified values of lift coefficient are for the propeller-removed condition and hence the values given for the tests with the propeller operating are somewhat lower than those actually obtained.

With the propeller removed the tests included measurements at yawed attitudes of  $0^\circ$  and  $-7.5^\circ$  for the two low lift conditions, and at yaws of  $-15^\circ$ ,  $-7.5^\circ$ , and  $0^\circ$  for the high lift coefficients. Tests were not made at the positive yaw attitudes with propeller removed as the canopy is symmetrical and the pressures at positive yaw should merely be in the opposite sense from those measured at negative yaws. With the propeller operating the power-off test procedure was repeated and was expanded to include additional tests for the same series of conditions throughout the positive yaw range. Thrust coefficients used in the tests to simulate constant military power operation in flight for each of the respective lift coefficients were determined from a flight curve of  $T_c$  against  $C_L$  for sea-level military power furnished by Grumman aircraft corporation (fig. 5). Tunnel-operation conditions for obtaining the proper  $T_c$  and  $C_L$  relationships for a constant airspeed of 60 miles per hour and constant propeller blade angle of  $26^\circ$  (0.75 radius) were obtained from a propeller calibration.

## SYMBOLS

$C_L$	lift coefficient $\left(\frac{L}{q_0 S}\right)$
$T_C$	thrust coefficient $\left(\frac{T}{\rho V^2 D^2}\right)$
$P$	pressure coefficient $\left(\frac{p - p_0}{q_0}\right)$
$L$	lift, pounds
$T$	thrust, pounds
$q_0$	free-stream dynamic pressure $\left(\frac{1}{2} \rho_0 V_0^2\right)$ , pounds per square foot
$\rho_0$	mass density of air, slugs per cubic foot
$p$	local static pressure, pounds per square foot
$p_0$	free-stream static pressure, pounds per square foot
$S$	wing area, square feet
$V$	airspeed, feet per second
$D$	propeller diameter, feet
$\psi$	angle of yaw, degrees

## Subscripts:

$i$	internal
$e$	external

## DISCUSSION OF RESULTS

The test results are presented in figures 6 to 13 in the form of pressure-distribution plots showing the variation of

external pressure coefficient  $\left(\frac{p - p_0}{q_0}\right)$  at four lateral stations

through the canopy (fig. 4) for each test condition. Internal static-pressure coefficients are also shown on the respective figures for each test condition. For all cases where the internal pressure is uniform an average value is shown and for conditions where the internal pressure varied the pressure coefficients at the four points of measurement are shown individually. The variation of internal pressure coefficient with yaw is shown in figure 14 for the complete range of airplane attitudes tested with propeller operating and canopy closed.

#### External Pressure Distribution

Zero yaw.— The results of tests made with the airplane at zero yaw are presented in figures 6 and 7. These results show that with propeller removed (fig. 6) the lateral distribution of pressure coefficient is symmetrical and has a maximum variation of approximately 0.25 from the sides to the top of the canopy. The highest negative pressure coefficients occur with the canopy closed or 3 inches open with maximum value of approximately  $0.70q_0$  reached over the top of the canopy. Neither the peak pressures nor the nature of the pressure distributions is appreciably affected by variation of lift coefficient.

With the propeller operating the test results show (fig. 7) that the magnitude of the pressure coefficient and the symmetry of distribution are appreciably affected at the higher thrust conditions due to the increased local velocity and rotation of the slipstream. For conditions with the propeller operating at low thrust coefficients (figs. 7(a) and 7(e)) the power effects are quite small. High thrust conditions, however, as shown by figures 7(b), 7(c), and 7(d), produce asymmetry of pressure distribution which results in a net side-load component to the right with maximum pressure coefficients as high as  $-1.8$  for the condition representing take-off with military power (fig. 7(d)). As seen from the test results (fig. 7), opening the canopy decreased the peak negative external pressure coefficient for any given condition by approximately 0.40 but resulted in increased pressure asymmetry at the front of the canopy.

Considering the external-internal pressure differential  $(P_e - P_i)$ , which is the basic parameter in determining net canopy exploding loads, the test results show that the greatest differential pressure exists with the canopy closed for all airplane attitudes investigated at zero yaw. Calculations indicate that the net loading for the high-speed attitude represented in figure 7(a) will be approximately double the loads encountered

in a military power take-off condition as represented by figure 7(d). Also, the loads encountered in a high-speed pull-up are expected to be approximately the same as those for the level-flight high-speed condition, inasmuch as the canopy pressures are not appreciably affected by increasing lift coefficient.

Negative yaw.— Figures 8 to 11 present the results of tests made with the airplane at negative yaw attitudes (right wing advanced). The results obtained with the propeller removed (figs. 8 and 9) show that yaw produces asymmetry in the pressure distributions with peak pressure coefficients reaching values as high as  $-1.1$  at a yaw angle of  $-15^\circ$ . The asymmetry is most pronounced at the front of the canopy although at the higher yaw attitudes (figs. 9(a) and 9(b)) appreciable asymmetry is in evidence at all four pressure-measurement stations. The propeller-removed results also show that variation of lift coefficient has only slight effects on the asymmetry of pressure distribution and magnitude of the peak negative pressures.

With the propeller operating (figs. 10 and 11) the results show that the lateral asymmetry of pressure is appreciably reduced inasmuch as the slipstream rotation tends to counteract the angle of flow over the canopy induced by negative yaw. At  $-7.5^\circ$  yaw attitude the slipstream effects at the higher thrust conditions (figs. 10(c) and 10(d)) completely overcome the asymmetry due to yaw. At  $-15^\circ$  yaw, however, the asymmetry due to yaw is never completely overcome although approximately symmetrical loading conditions are indicated for the high thrust condition (fig. 11(b)). For all negative yaw conditions the external pressure coefficients have the greatest negative values with the canopy closed or 3 inches open but show the greatest asymmetry of distribution with the canopy full open. The test results indicate that the net canopy exploding force based on external-internal pressure differential ( $P_e - P_i$ ) will be greatest with canopy closed for all negative yaw attitudes.

Positive yaw.— The results of tests made at positive yaw attitudes (right wing retarded) with propeller operating are presented in figures 12 and 13. These results show that at positive yaw attitudes the effects of slipstream rotation and yaw combine to cause very pronounced asymmetry and high negative peaks in the lateral pressure distributions. As shown for negative yaw conditions the lateral asymmetry of pressure is most pronounced at the front sections of the canopy and the greatest negative pressures occur on these sections. The pressure asymmetry is similar to that shown at negative yaw attitudes in that the location of section peak negative pressures vary from front to rear. In general for the canopy-closed condition, the negative pressure peaks at the front of the canopy (station 1) occur

approximately over tube number 5 on the side near the retarded wing, and for the rear stations the peaks progressively shift so that for station 4 the negative pressure peak is approximately over tube number 3 on the side near the advancing wing.

The nature of the distribution of side forces on the canopy due to the pressure asymmetry will be similar to that discussed for zero yaw conditions except that it is more extreme. Based on external-internal pressure differential ( $P_e - P_i$ ), the results indicate that the net exploding forces will be greatest with canopy closed throughout the positive yaw range. As noted at zero and negative yaw attitudes, the effect of opening the canopy is to decrease the magnitude of the external negative pressures and increase the internal negative pressures. Calculations indicate that although maximum negative pressures as high as  $-3.0q_0$  are encountered in the worst conditions at  $15^\circ$  positive yaw (fig. 13(b)), the over-all net exploding force on the canopy should not exceed that for the high-speed attitude with zero yaw.

#### Internal Static Pressures

Static pressures measured at the inner surface of the canopy are shown in conjunction with the external pressure distributions presented in figures 6 to 13 for the complete range of test conditions. In addition, figure 14 is presented to summarize the variation of internal pressure coefficient with yaw angle for all the tests made with canopy closed and propeller operating. From the test results it is seen that the internal pressure has a negative value throughout the range of conditions investigated. The least negative value of internal pressure coefficient measured was  $-0.15$  for the high-speed attitude ( $C_L, 0.20$ ;  $T_C, 0.04$ ) with canopy closed (fig. 14). The effect of increasing lift coefficient with propeller operating at thrust coefficients simulating military power was to decrease the internal pressure coefficient as shown by figure 14. The effect of airplane yaw also is to reduce slightly the internal pressures at the higher angles of yaw when the thrust coefficient is small and to a considerably greater extent when the thrust coefficient is high. These results show that the variation of internal pressure coefficient is a direct reflection of the external-pressure-field variation and the cockpit leakage; therefore, any variable which causes the external pressures to become more negative has the same effect on the internal pressures. Likewise partially opening the canopy increases the leakage area and allows air to flow freely from the inside of the cockpit to the surrounding lower pressure area, thus causing the further reduction in internal pressure shown for canopy positions from closed to half open.

For the canopy full-open position, however, this trend is reversed and the internal pressure becomes less negative as air is probably flowing under the canopy for this condition. For all tests at zero and negative yaw attitudes the internal pressure is uniform throughout the canopy. At the positive yaw attitudes with propeller operating (Figs. 12 and 13) and canopy open the internal pressures become quite irregular due to the influence of the asymmetrical external pressure field and disturbed flow conditions.

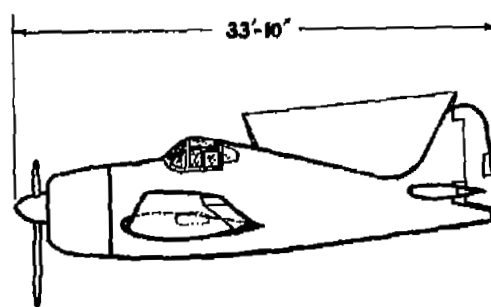
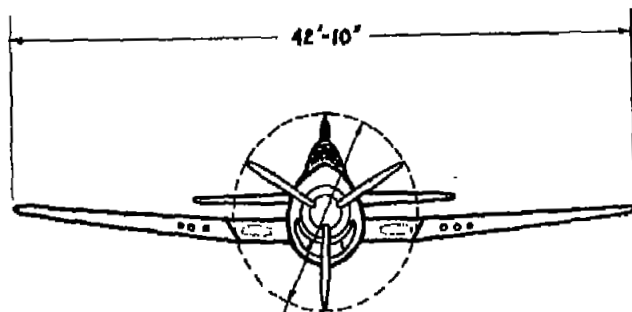
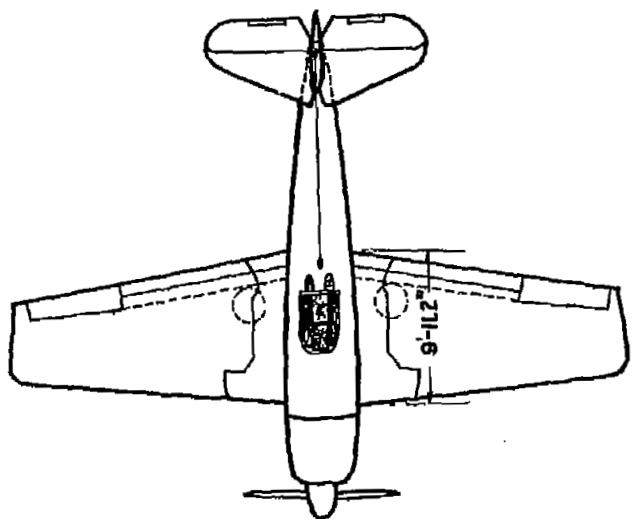
#### CONCLUDING REMARKS

The results of the investigation of pressure distributions on the conventional single-place canopy of the Grumman F6F-3 airplane show that:

1. The net exploding forces on the canopy will be greatest when the airplane is operating at high speed with canopy closed.
2. For all conditions the net canopy load will be in an exploding direction.
3. At all attitudes investigated, partially opening the canopy reduces the external-internal pressure differential, thus reducing the net exploding loads.
4. Yawing the airplane increases the magnitude of the peak negative pressure coefficients and results in an asymmetrical lateral distribution of pressure which becomes more pronounced with increasing yaw.
5. The high axial velocities and rotation of the slipstream at high thrust conditions also increase the magnitude of the pressure coefficient and produce asymmetry in the distribution of pressure. The effects of propeller operation are most pronounced at positive yaw attitudes as the flow asymmetry due to clockwise slipstream rotation combines with the flow asymmetry due to positive yaw.
6. Varying the lift coefficient has little effect on either the asymmetry or magnitude of the pressure coefficients.

Langley Memorial Aeronautical Laboratory  
National Advisory Committee for Aeronautics  
Langley Field, Va.

Weight ----- 11,441 lb  
 Wing section  
     Root ----- NACA 23015.6 (Modified)  
     Tip ----- NACA 23009  
 Wing area ----- 334.0 sq ft  
 Twin-row two-stage-supercharged engine  
 1650 hp at 2700 rpm at 25,000 ft  
 Propeller gear ratio ----- 2:1



NATIONAL ADVISORY  
 COMMITTEE FOR AERONAUTICS

18'-1" DIAM.

Figure 1 - Three-view drawing of the Grumman F6F-3 airplane

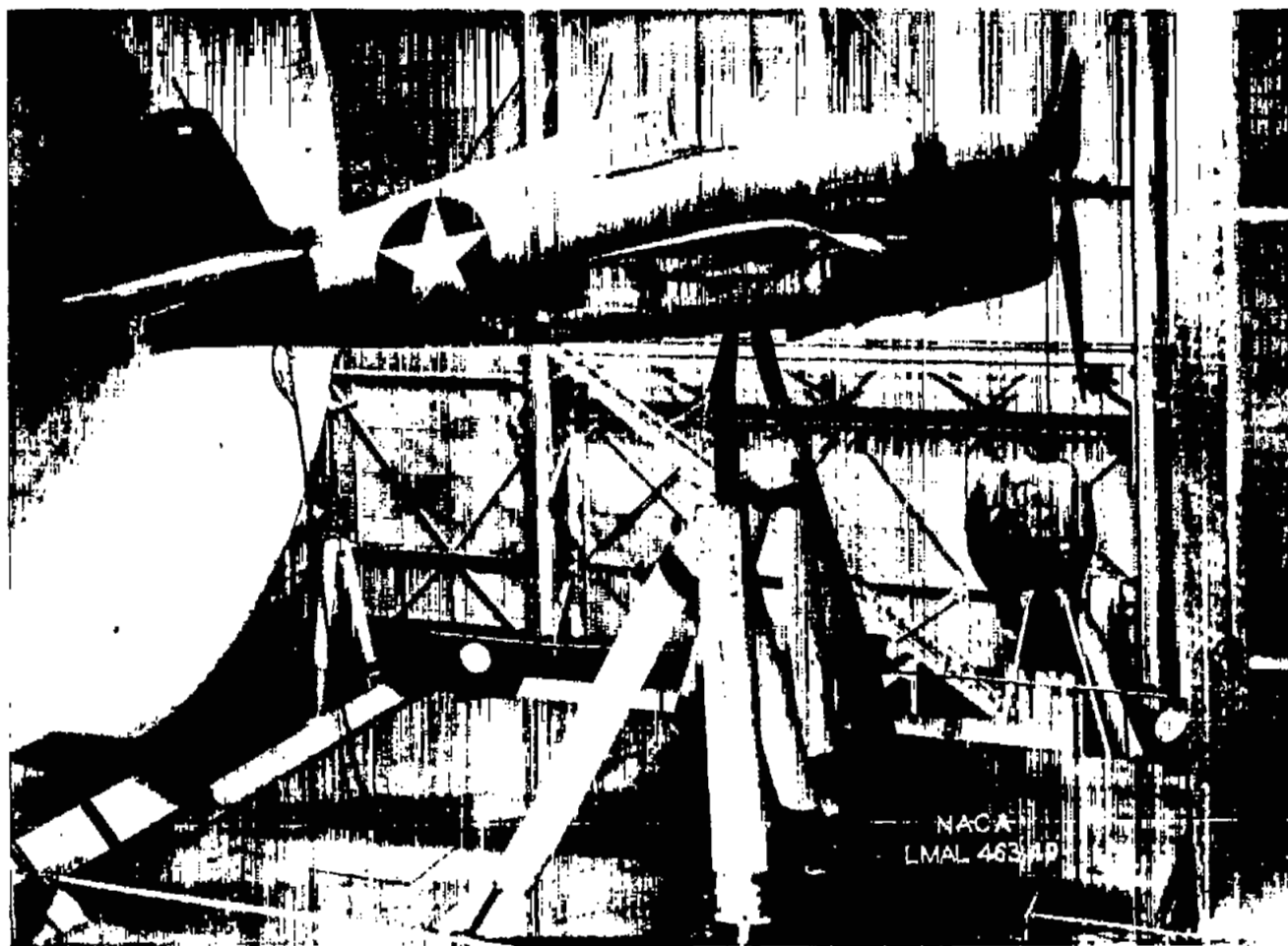


Figure 2.- The F6F-3 airplane mounted in the full-scale tunnel.

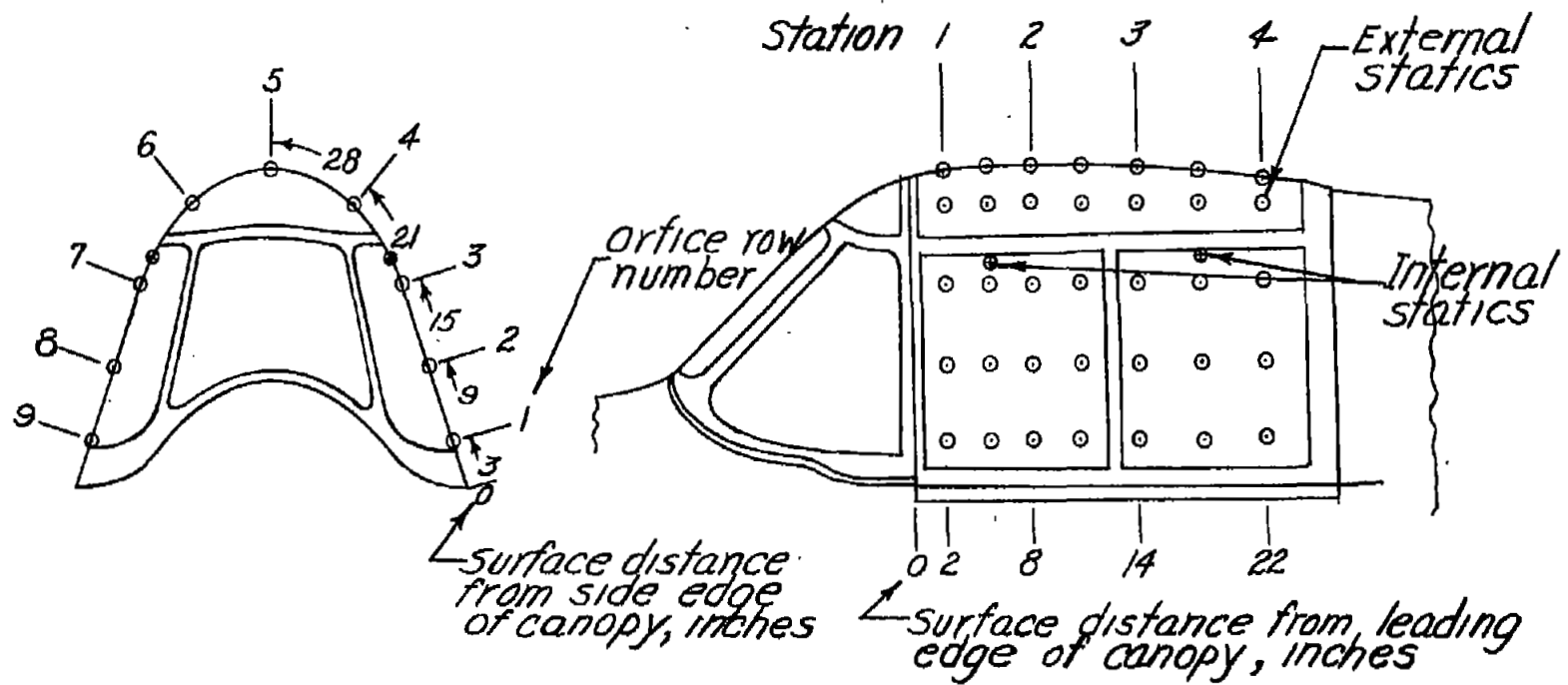


(a) Canopy closed.



(b) Canopy full open.

Figure 3.- Photographs showing the general arrangement of the F6F-3 cockpit canopy.



NATIONAL ADVISORY  
COMMITTEE FOR AERONAUTICS

Figure 4.-Static pressure orifice locations in the F6F-3 cockpit canopy.

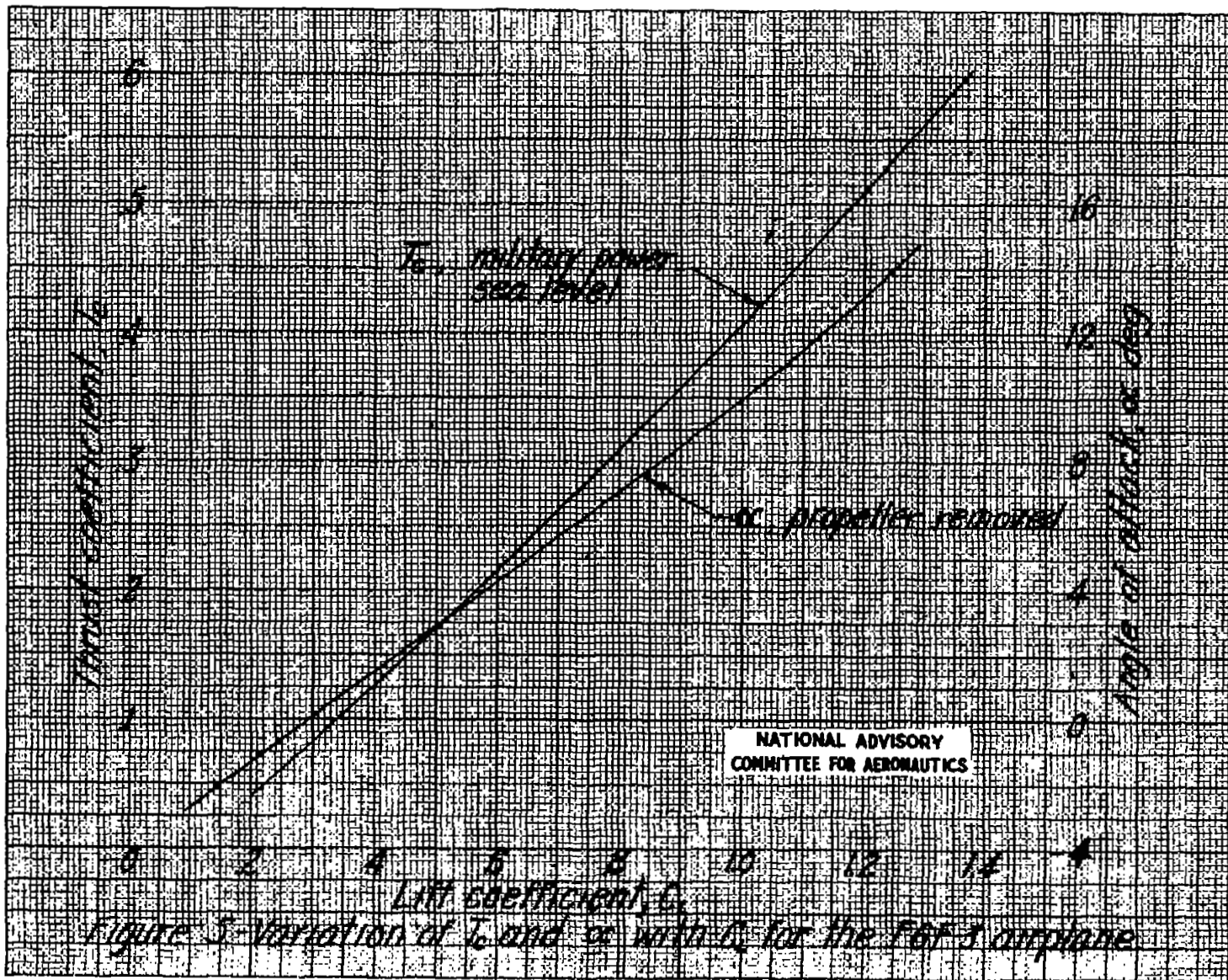
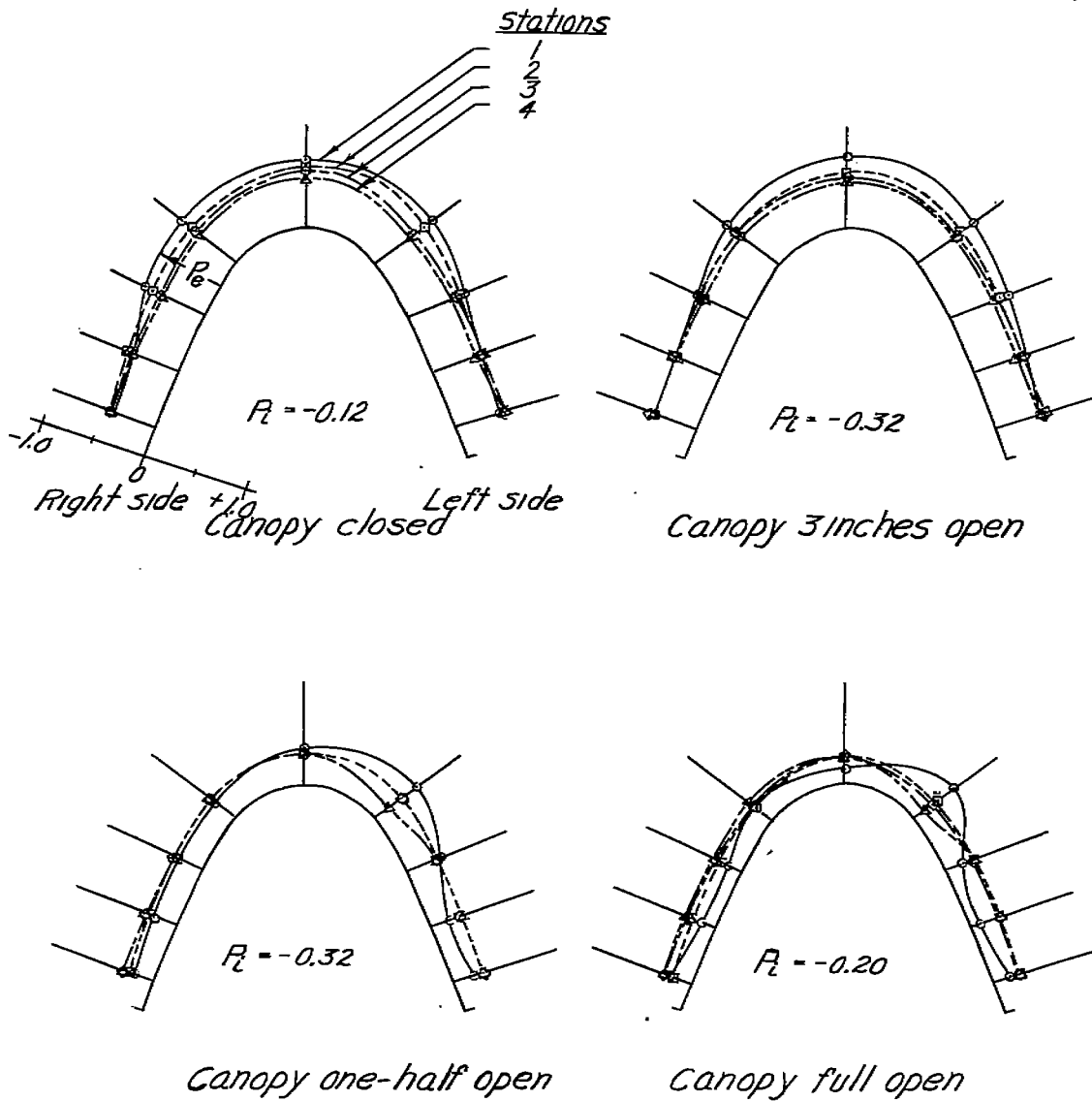


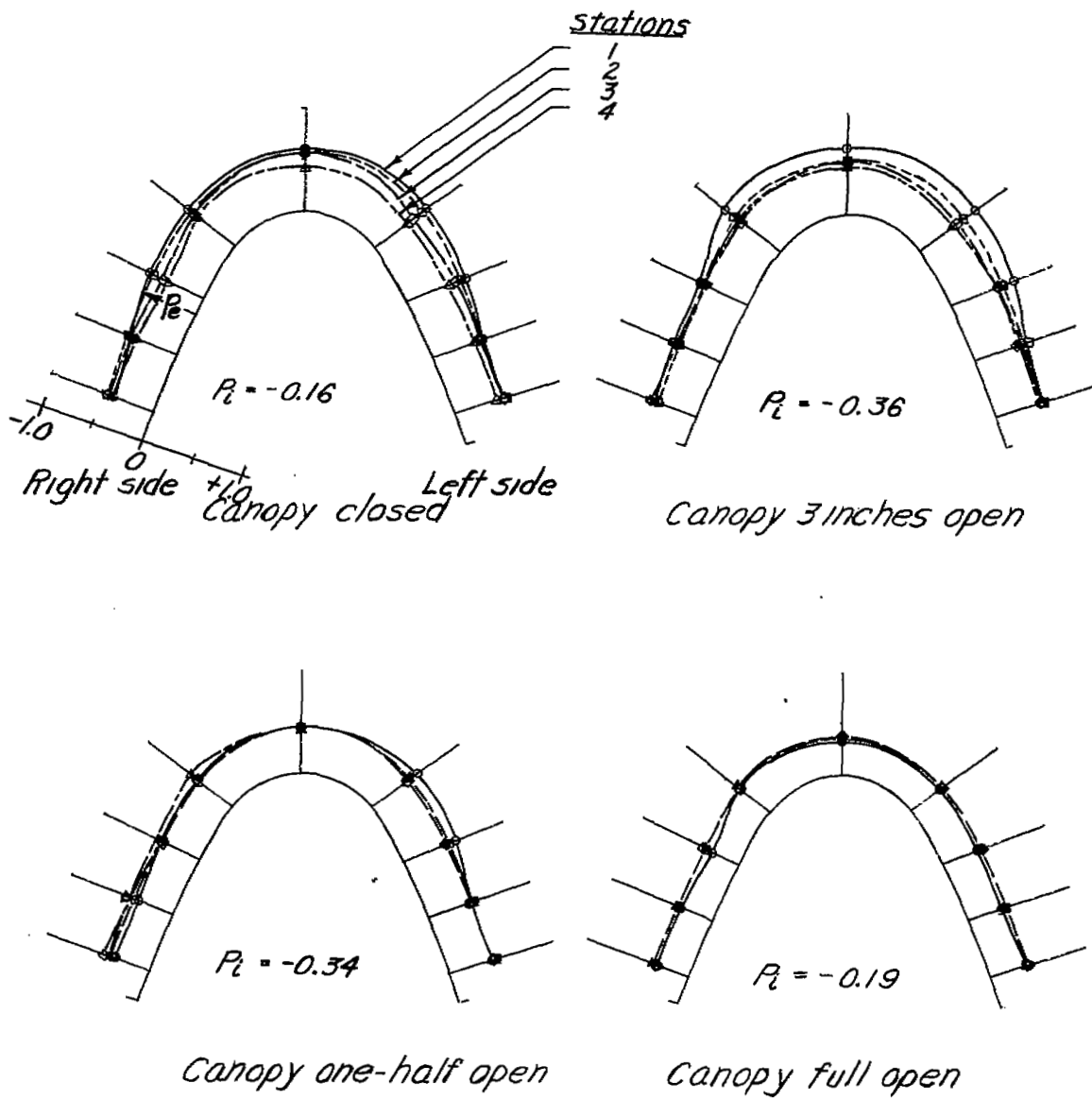
Figure 5-Variation of  $T_m$  and  $P_{ac}$  with  $C_L$  for the F6F-3 airplane



NATIONAL ADVISORY  
COMMITTEE FOR AERONAUTICS

(a) Propeller removed;  $C_L, 0.20$

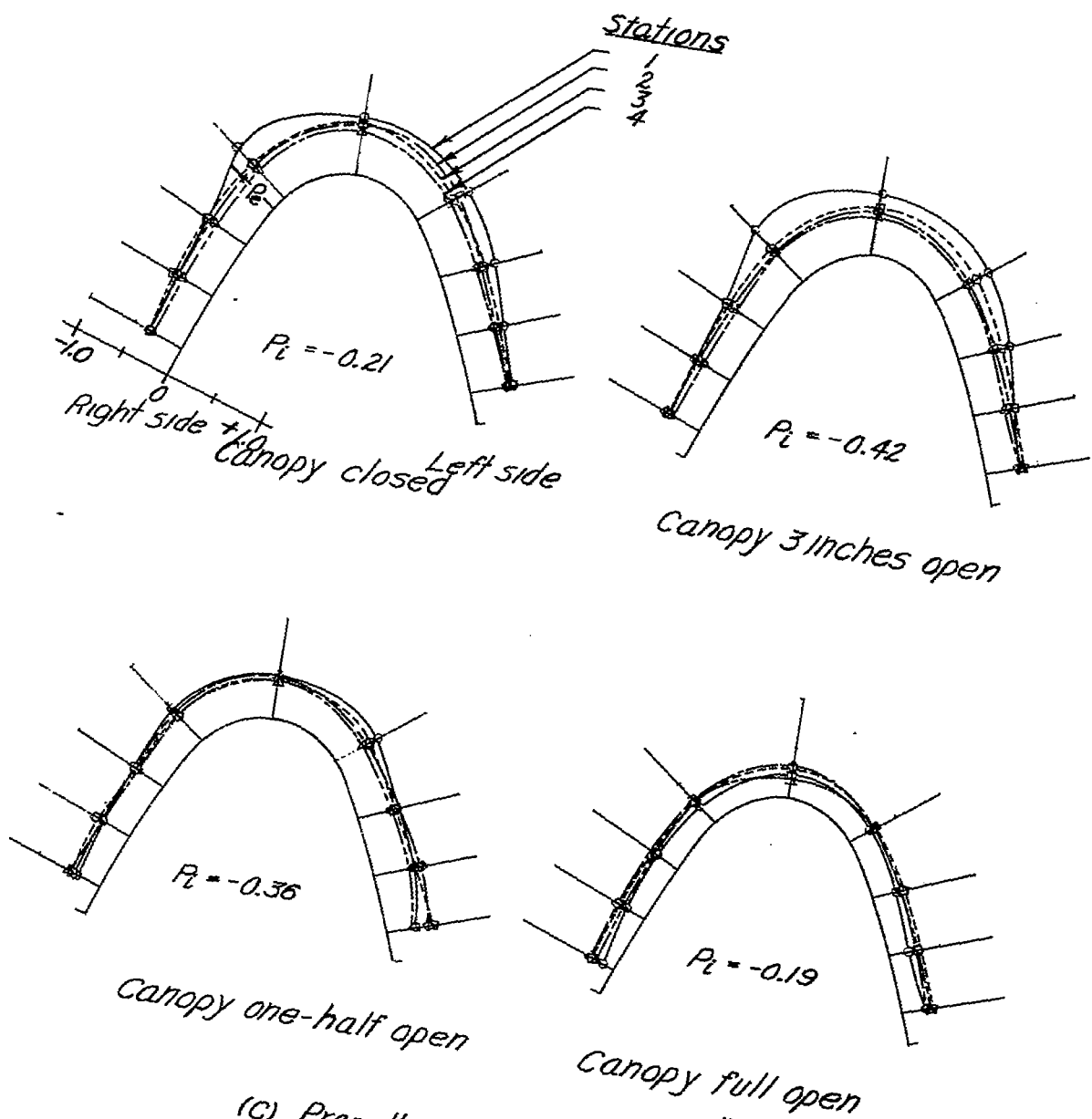
Figure 6. - Pressure distributions over the canopy of the F6F-3 airplane.  $\psi, 0^\circ$



NATIONAL ADVISORY  
COMMITTEE FOR AERONAUTICS

(b) Propeller removed;  $C_L, 0.52$

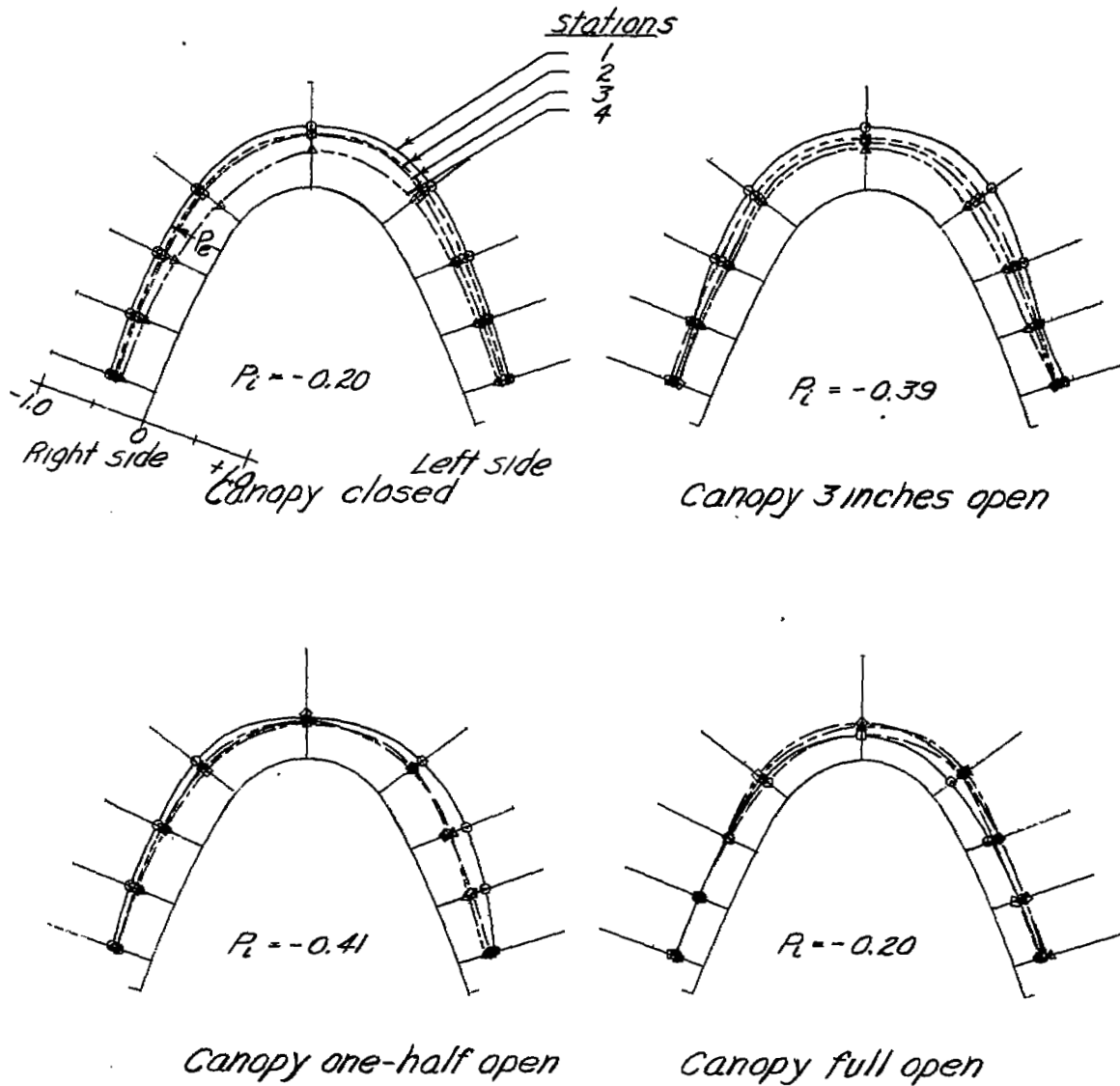
Figure 6.- continued.



(c) Propeller removed;  $C_L, 0.91$

Figure 6.- continued.

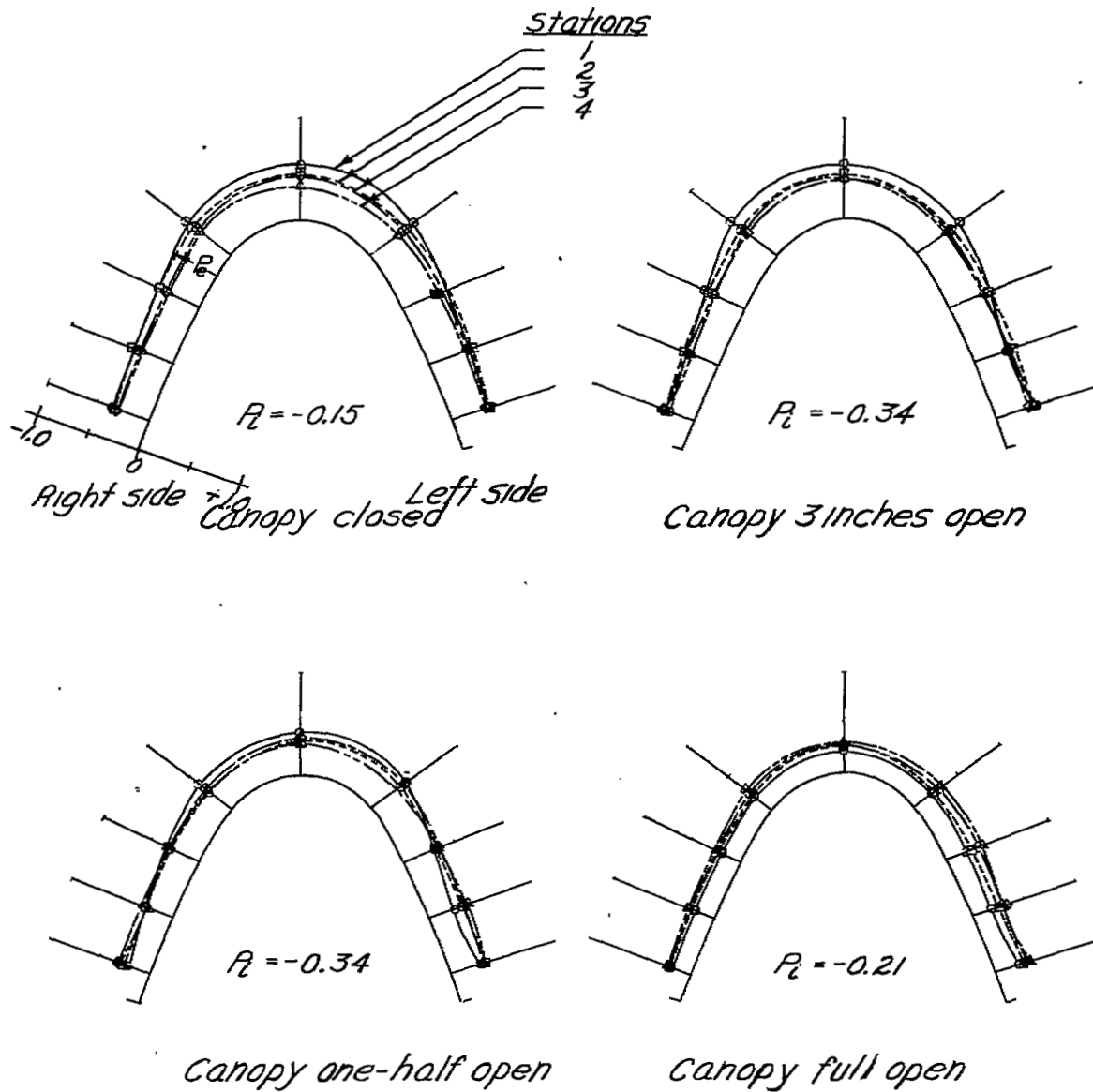
NATIONAL ADVISORY  
COMMITTEE FOR AERONAUTICS



NATIONAL ADVISORY  
COMMITTEE FOR AERONAUTICS

(d) Propeller removed;  $C_L, 1.23$

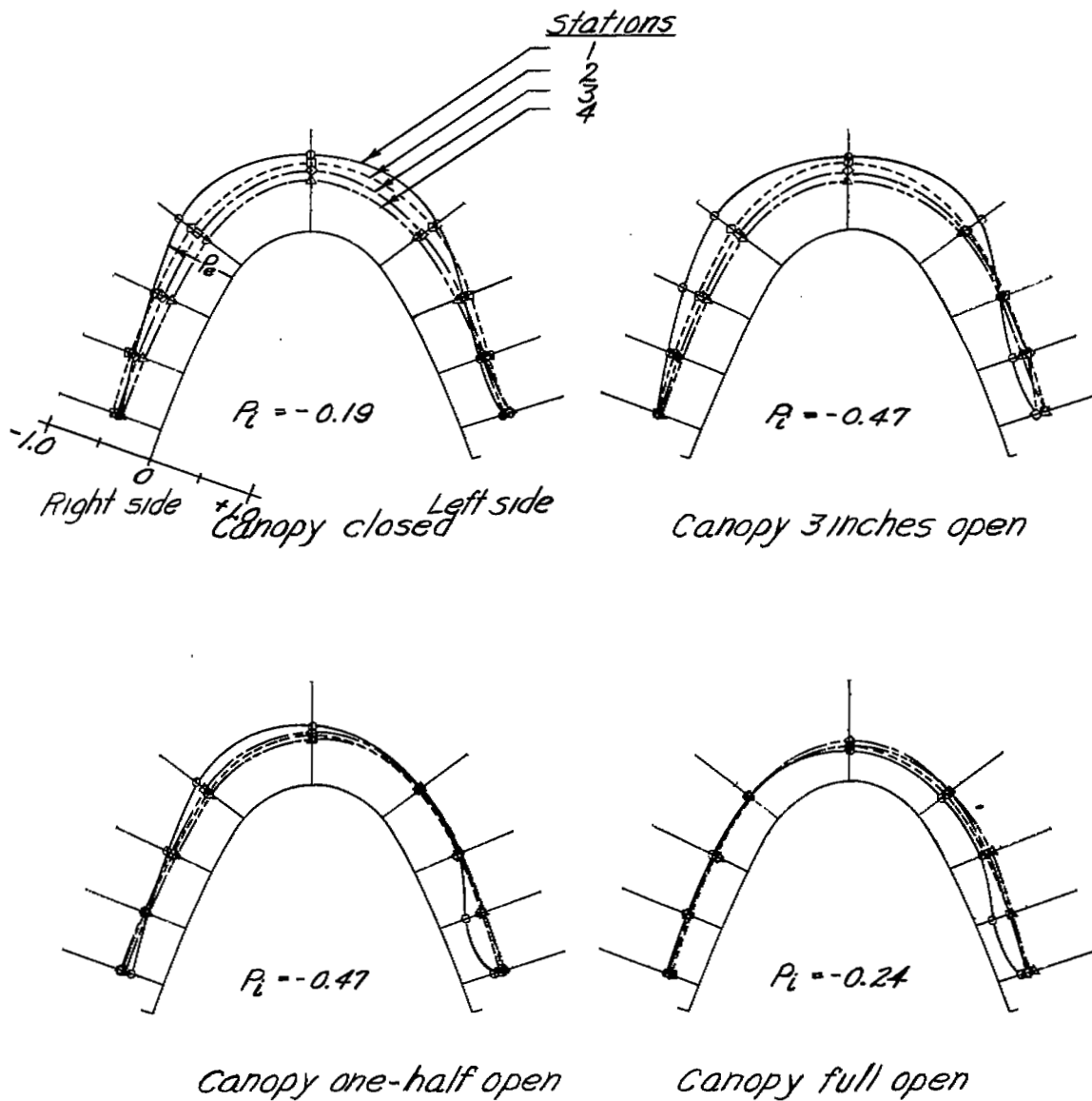
Figure 6.- concluded.



NATIONAL ADVISORY  
COMMITTEE FOR AERONAUTICS

(a) Military power;  $T_c, 0.04$ ;  $C_L, 0.20$

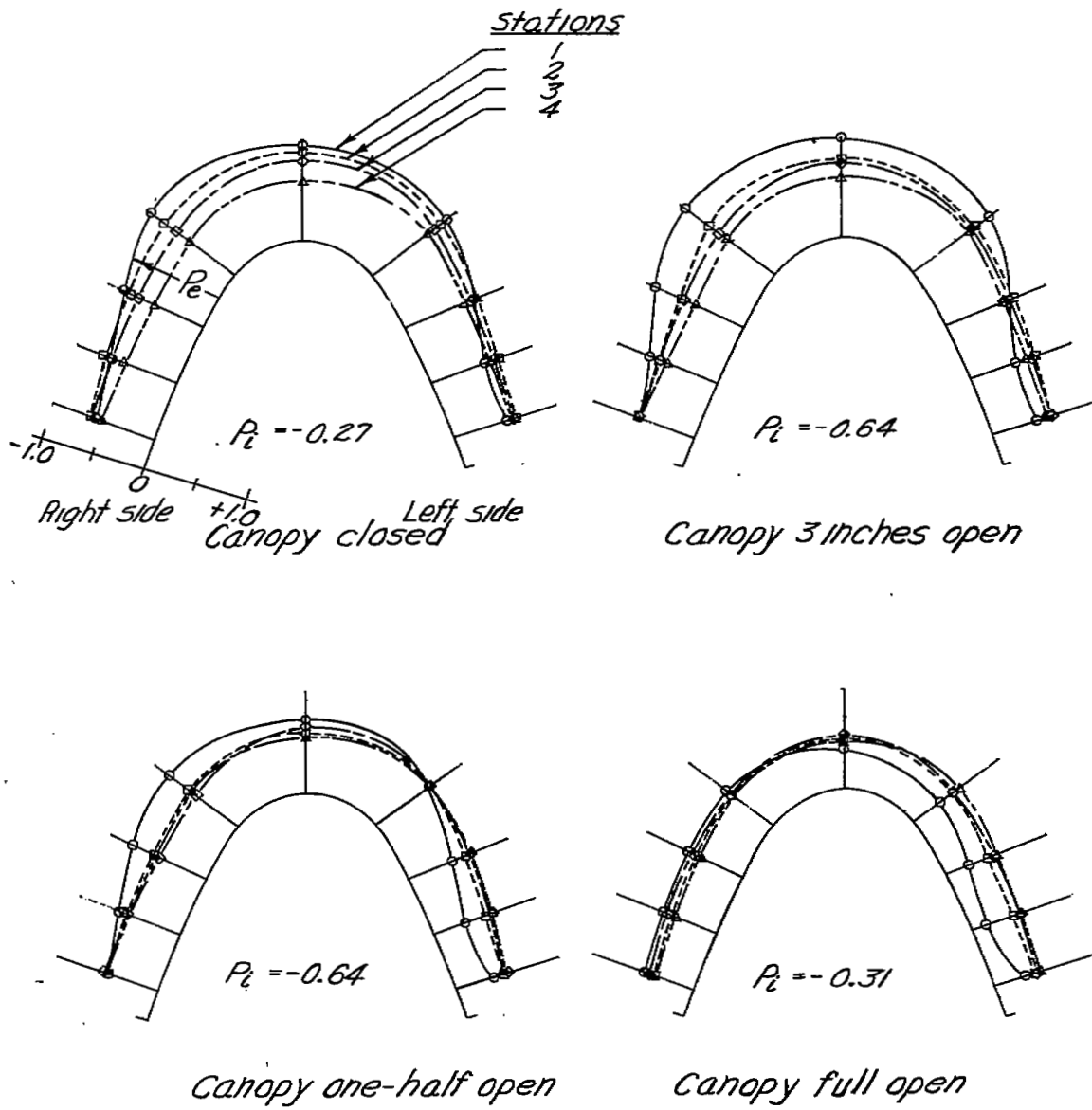
Figure 7. - Pressure distributions over the canopy of the F6F-3 airplane.  $\Psi, 0^\circ$



NATIONAL ADVISORY  
COMMITTEE FOR AERONAUTICS

(b) Military power;  $T_c, 0.18$ ;  $C_L, 0.52$

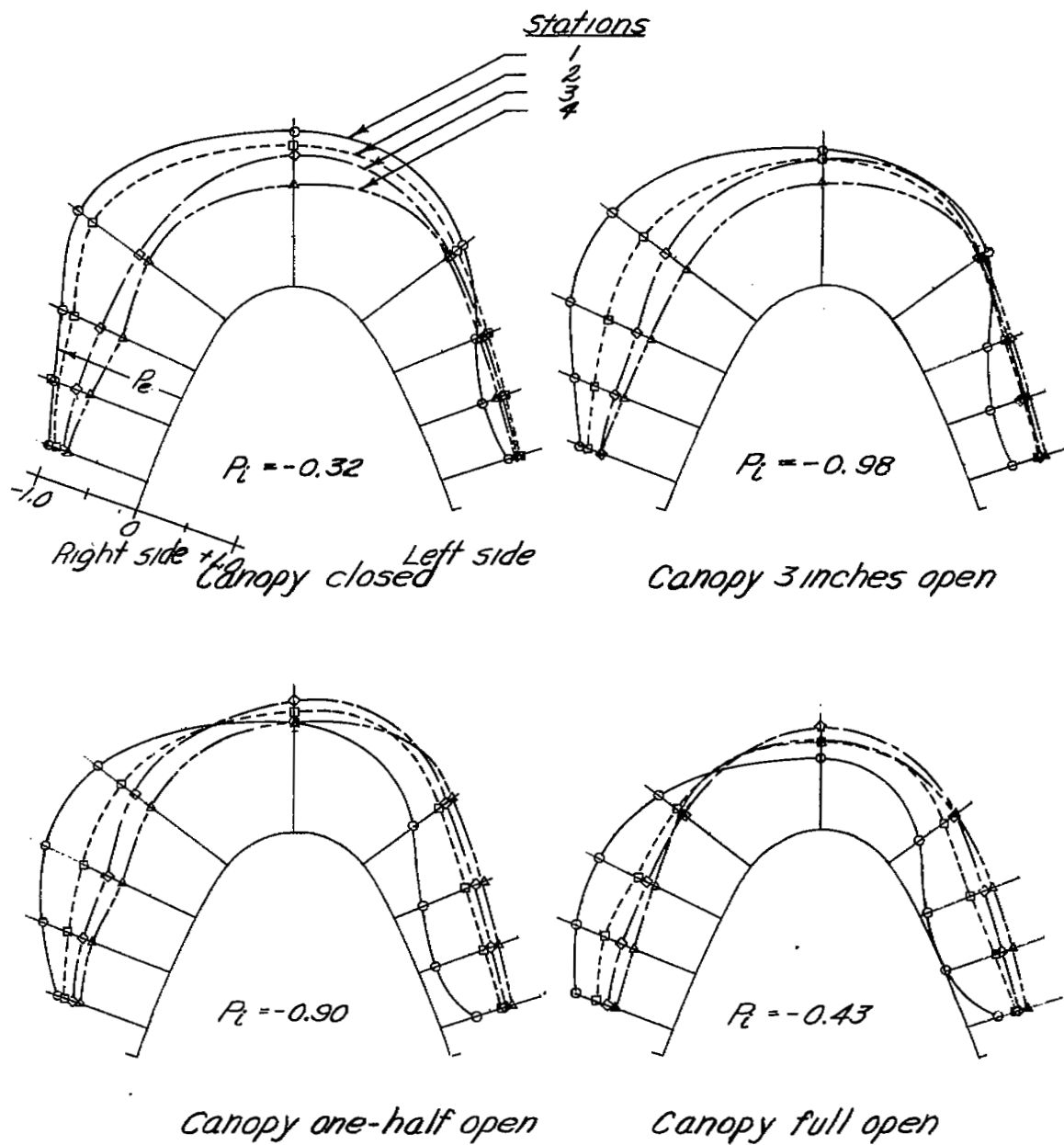
Figure 7.— continued.



NATIONAL ADVISORY  
COMMITTEE FOR AERONAUTICS

(c) Military power;  $T_c, 0.36$ ;  $C_L, 0.91$ .

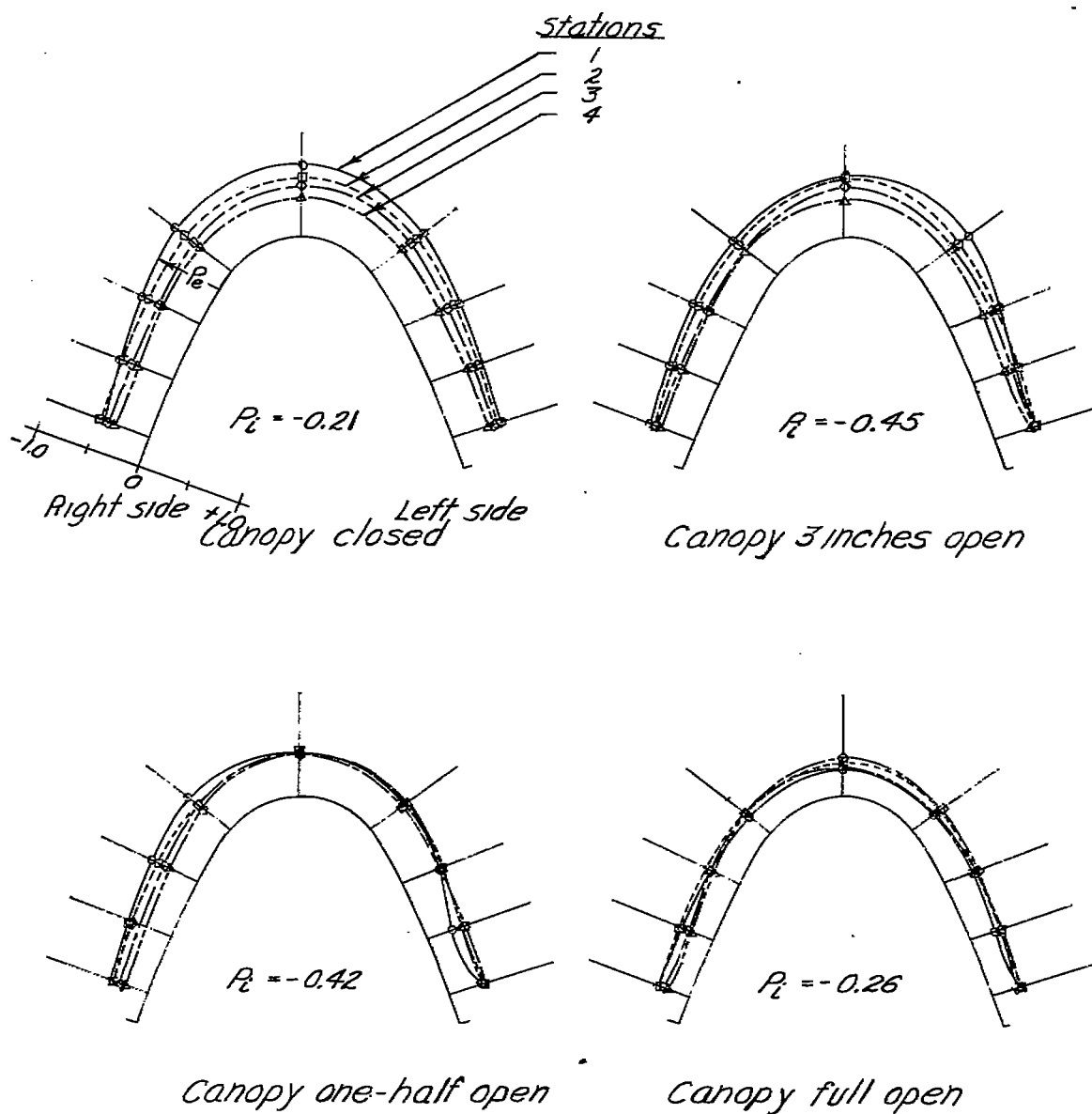
Figure 7.— continued.



NATIONAL ADVISORY  
COMMITTEE FOR AERONAUTICS

(d) Military power;  $T_c, 0.53$ ;  $C_L, 1.23$

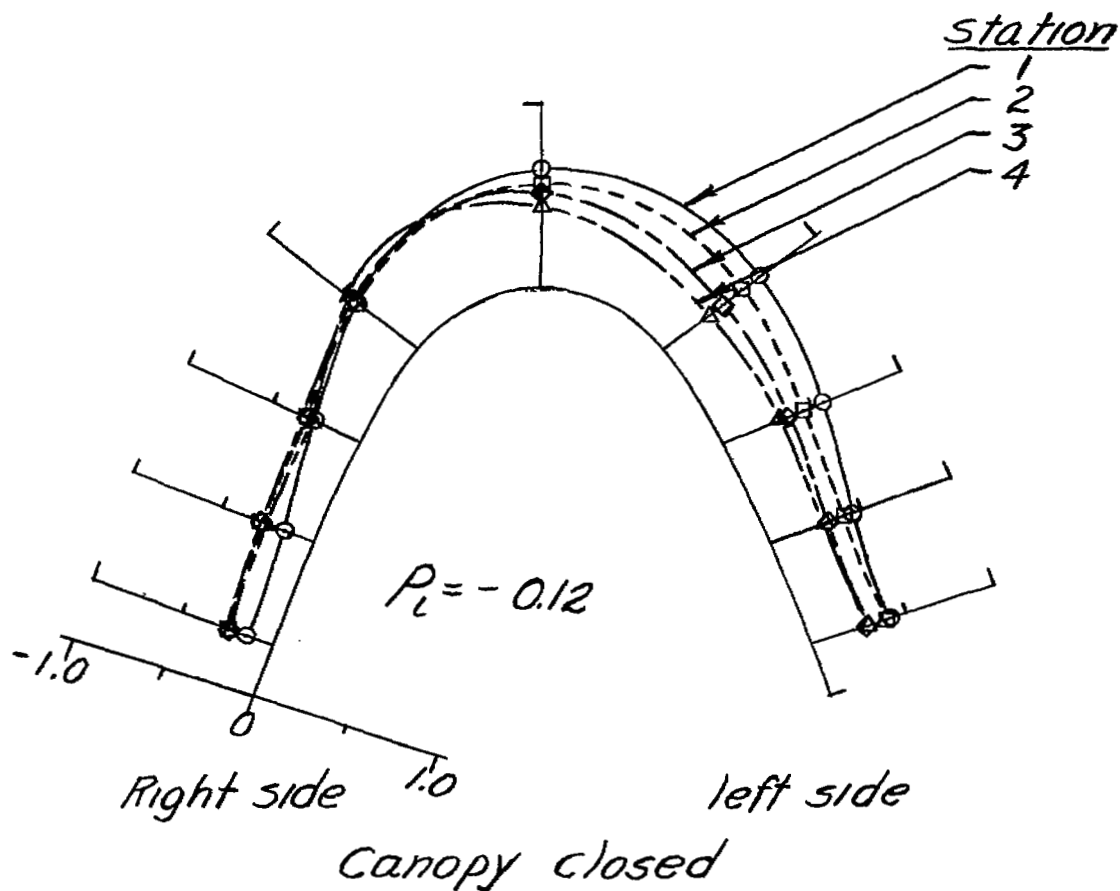
Figure 7. - continued.



NATIONAL ADVISORY  
COMMITTEE FOR AERONAUTICS

(e) Propeller idling;  $C_L, 1.23$

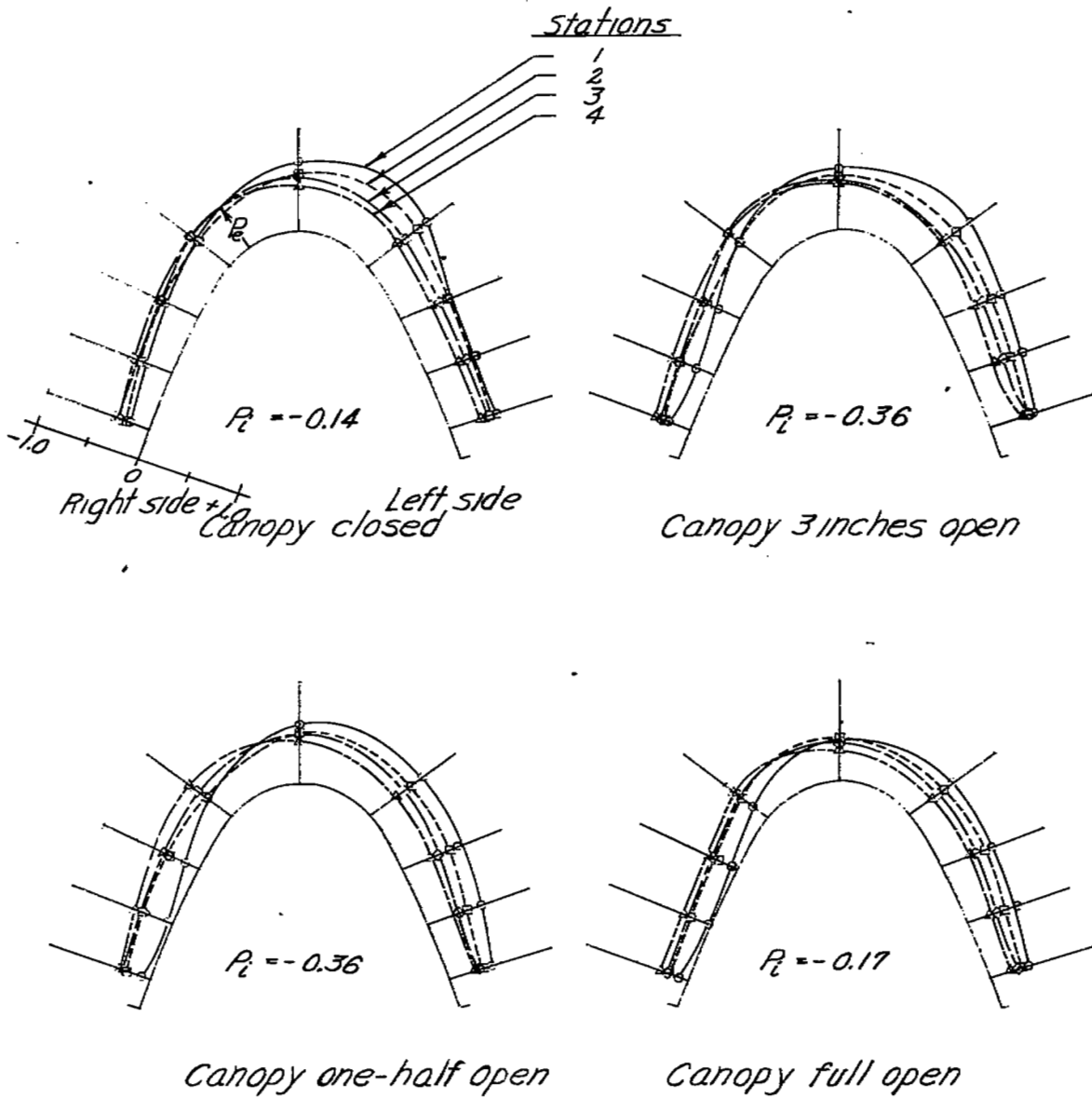
Figure 7.- concluded.



NATIONAL ADVISORY  
COMMITTEE FOR AERONAUTICS

(a) Propeller removed;  $C_L, 0.20$

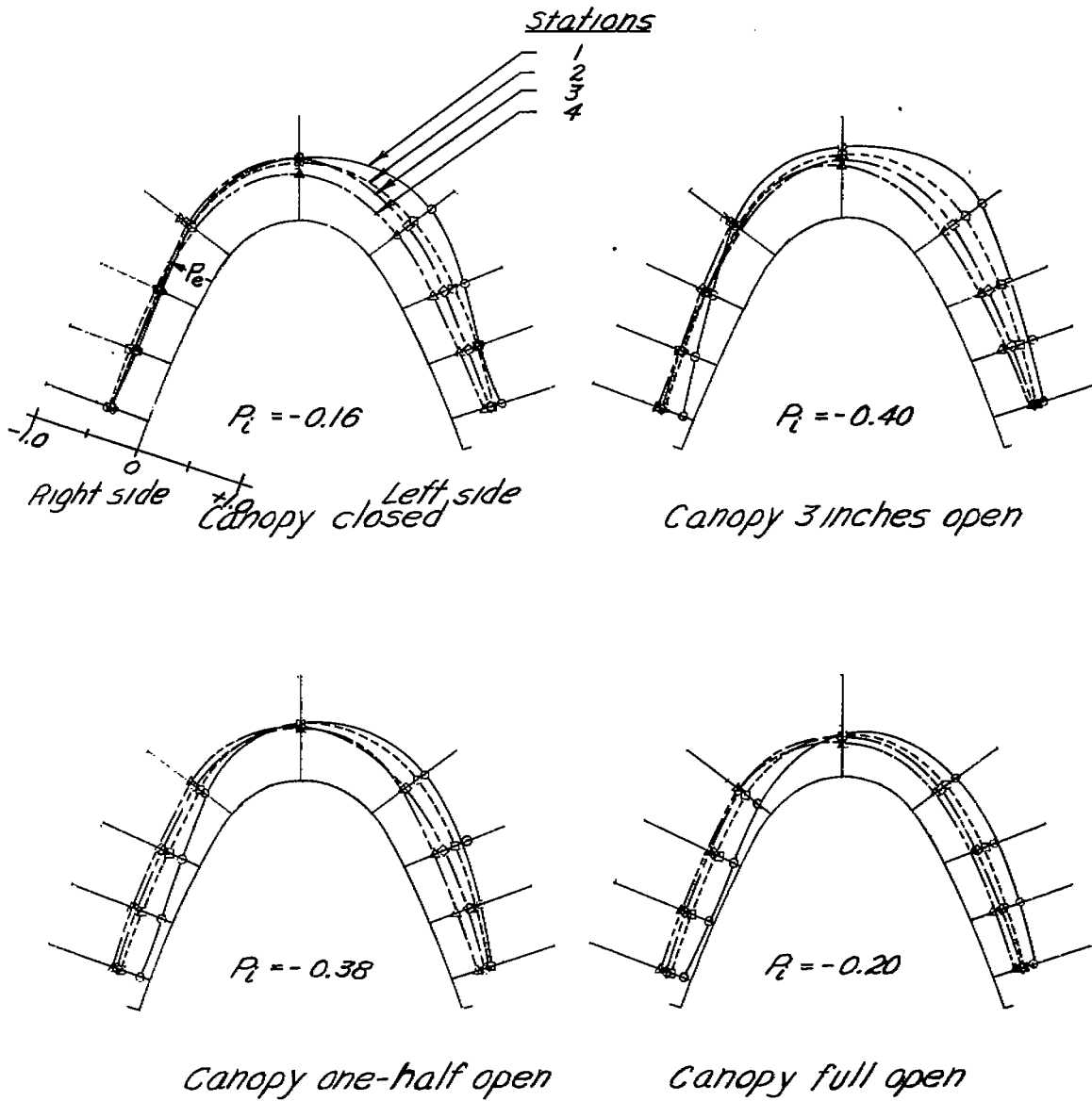
Figure 8.- Pressure distributions over  
the canopy of the F6F-3  
airplane.  $\psi, -7.5^\circ$



NATIONAL ADVISORY  
COMMITTEE FOR AERONAUTICS

(b) Propeller removed;  $C_L, 0.52$

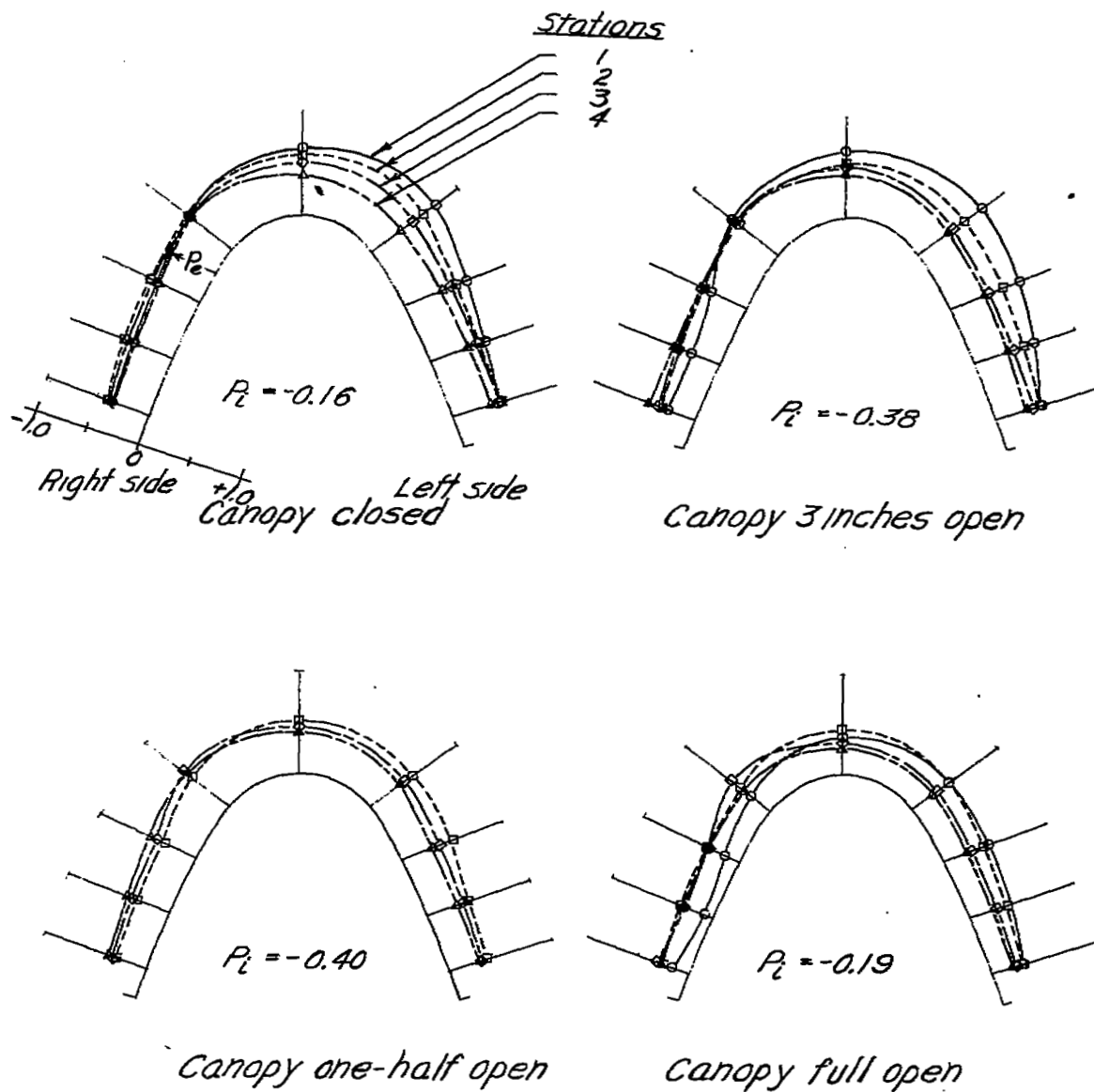
Figure 8.- continued.



NATIONAL ADVISORY  
COMMITTEE FOR AERONAUTICS

(c) Propeller removed;  $C_L, 0.91$

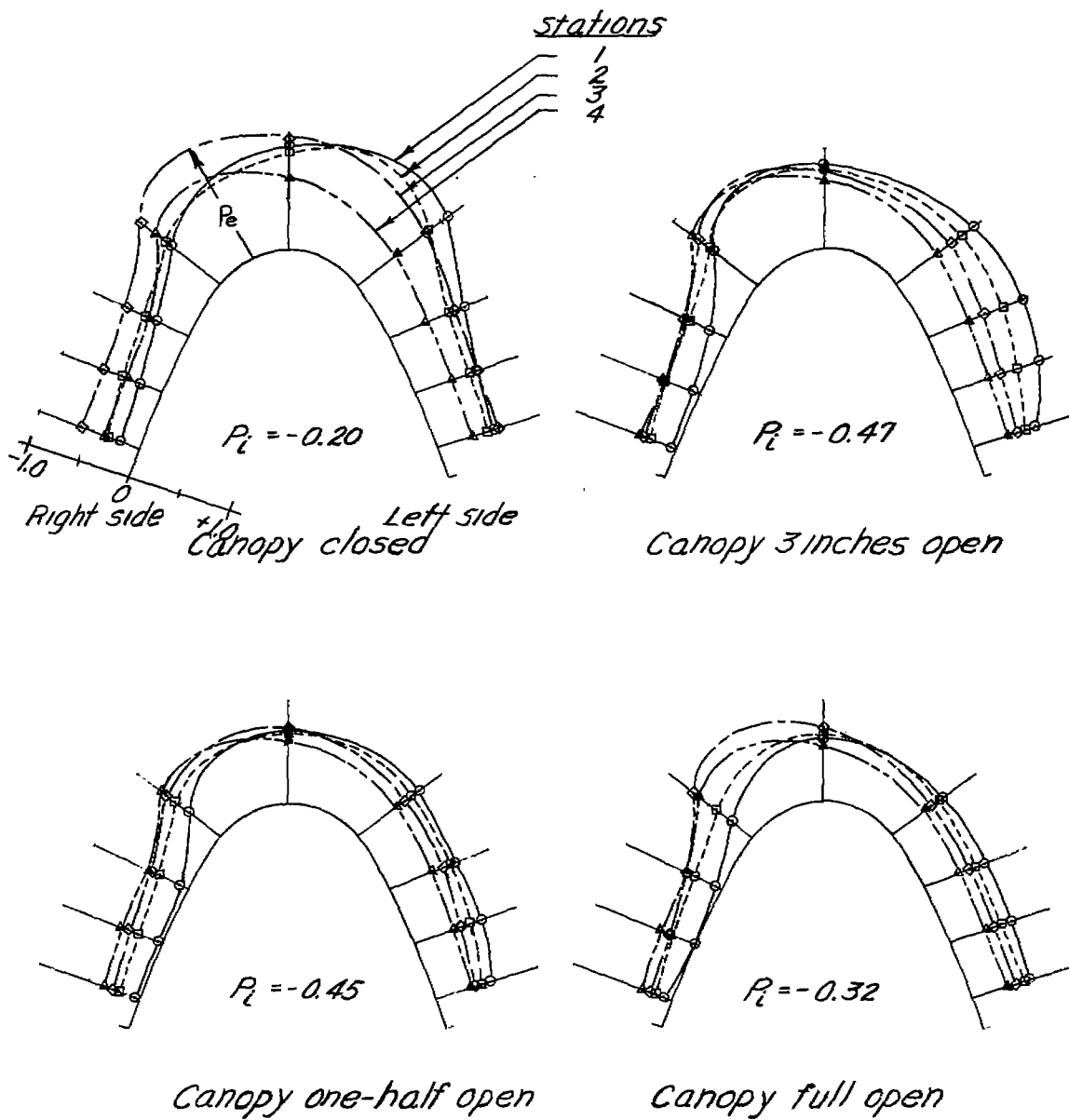
Figure 8. - continued.



NATIONAL ADVISORY  
COMMITTEE FOR AERONAUTICS

(d) Propeller removed;  $C_L, 1.23$

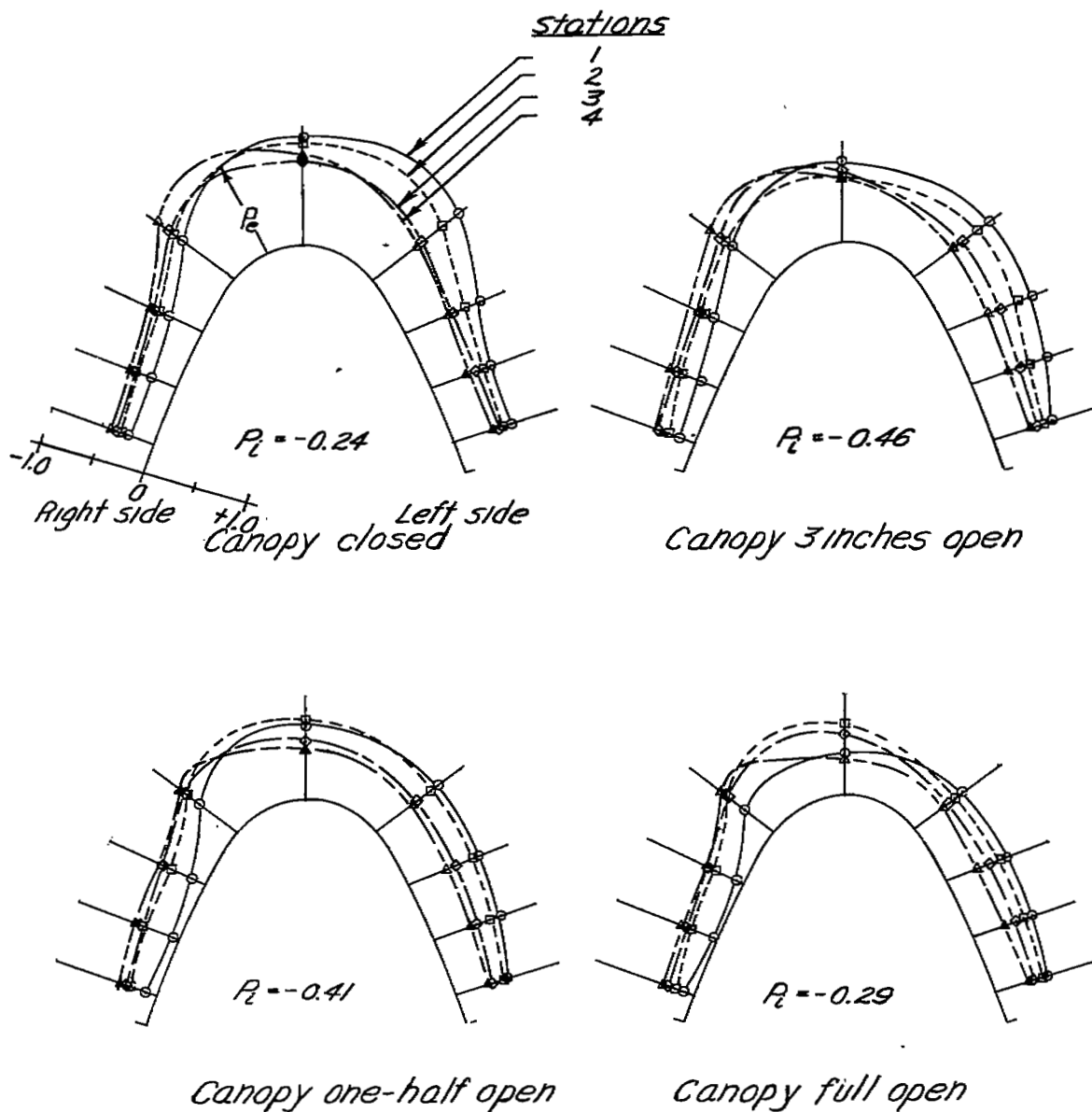
Figure 8. - concluded.



NATIONAL ADVISORY  
COMMITTEE FOR AERONAUTICS

(a) Propeller removed;  $C_L, 0.91$

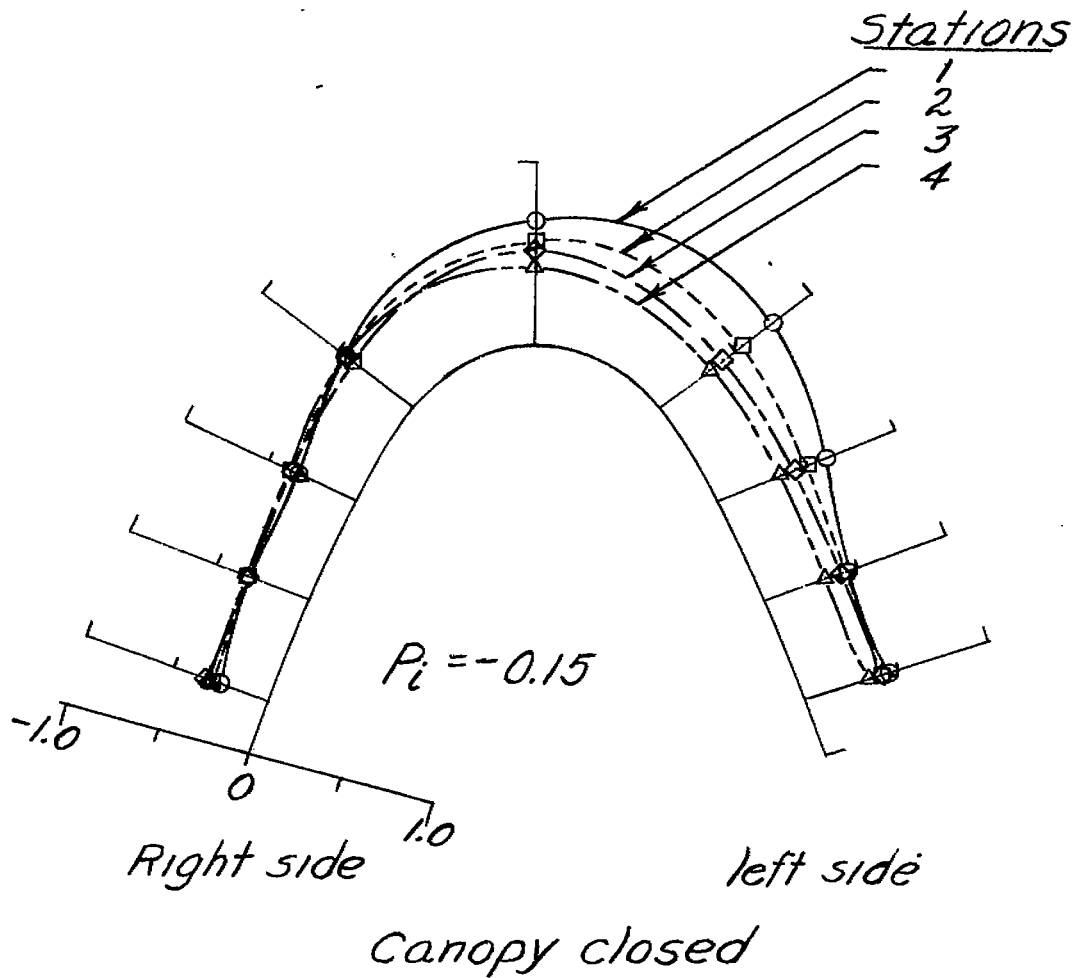
Figure 9 - Pressure distributions over the canopy of the F6F-3 airplane.  $\psi, 15^\circ$



NATIONAL ADVISORY  
COMMITTEE FOR AERONAUTICS

(b) Propeller removed;  $C_L, 1.23$

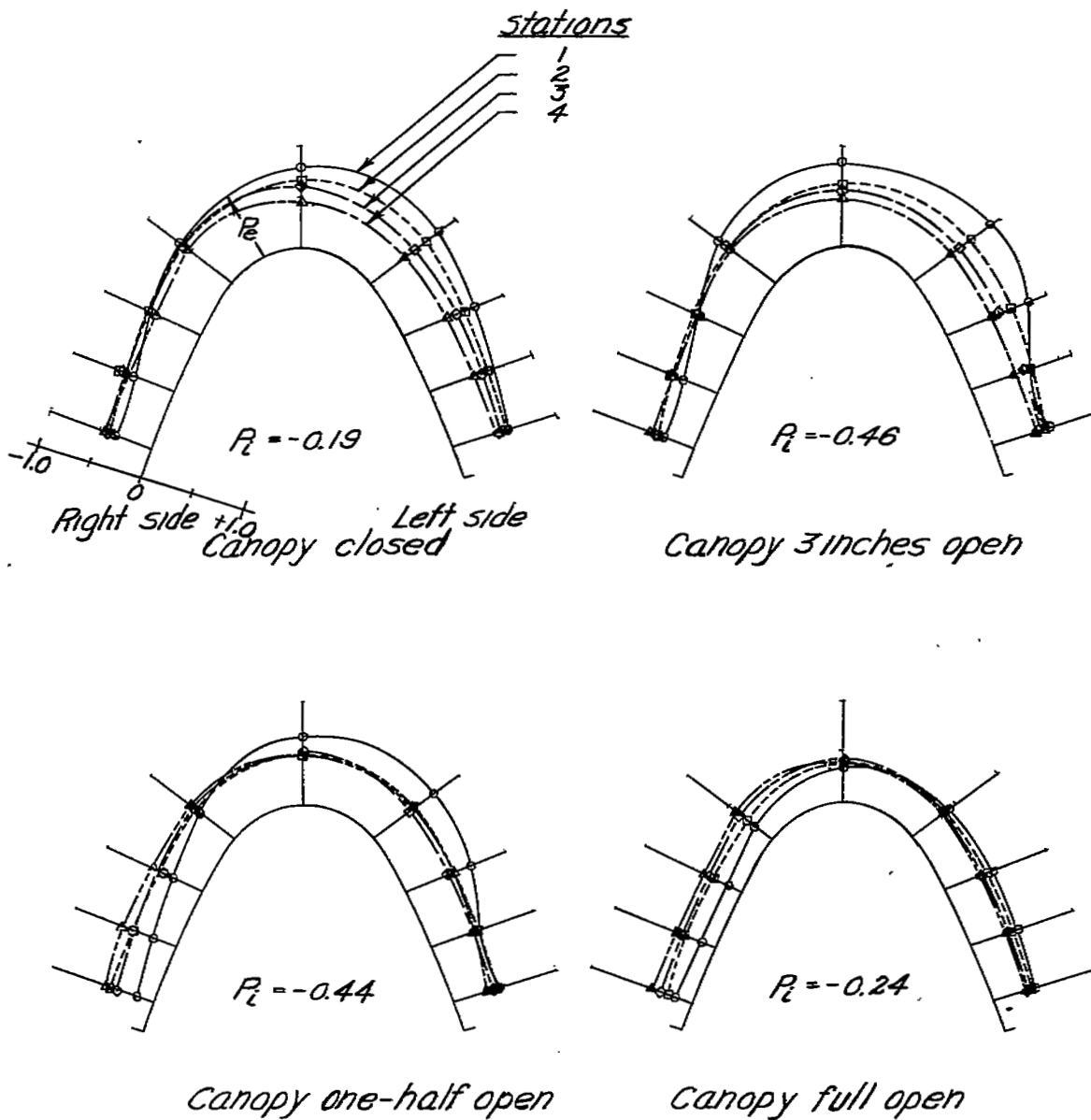
Figure 9.- concluded.



NATIONAL ADVISORY  
COMMITTEE FOR AERONAUTICS

(a) Military power;  $T_c, 0.04$ ;  $C_L, 0.20$

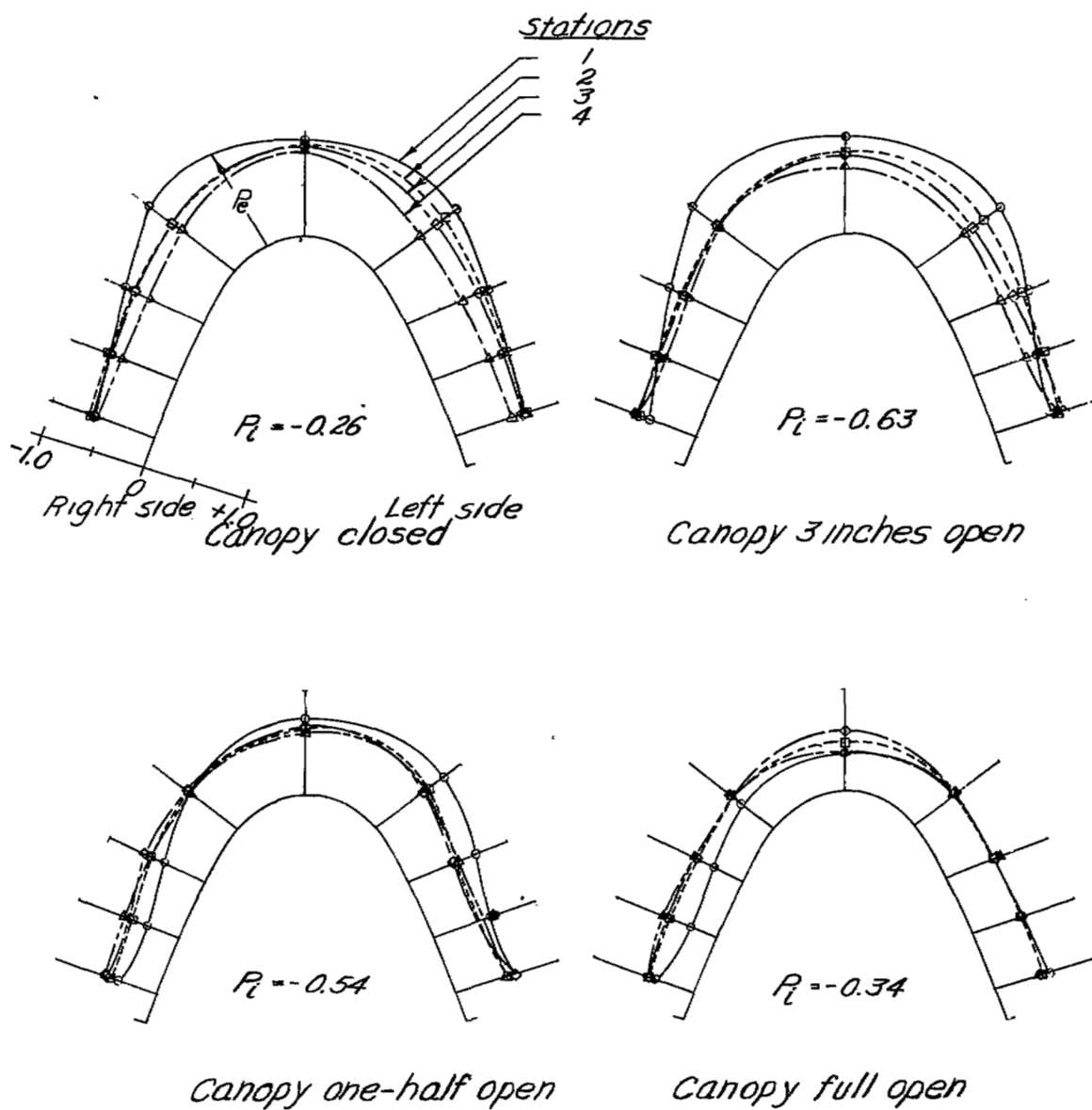
Figure 10.- Pressure distributions over the canopy of the F6F-3 airplane.  $\psi, -7.5^\circ$



NATIONAL ADVISORY  
COMMITTEE FOR AERONAUTICS

(b) Military power;  $T_0, 0.18$ ;  $C_L, 0.52$

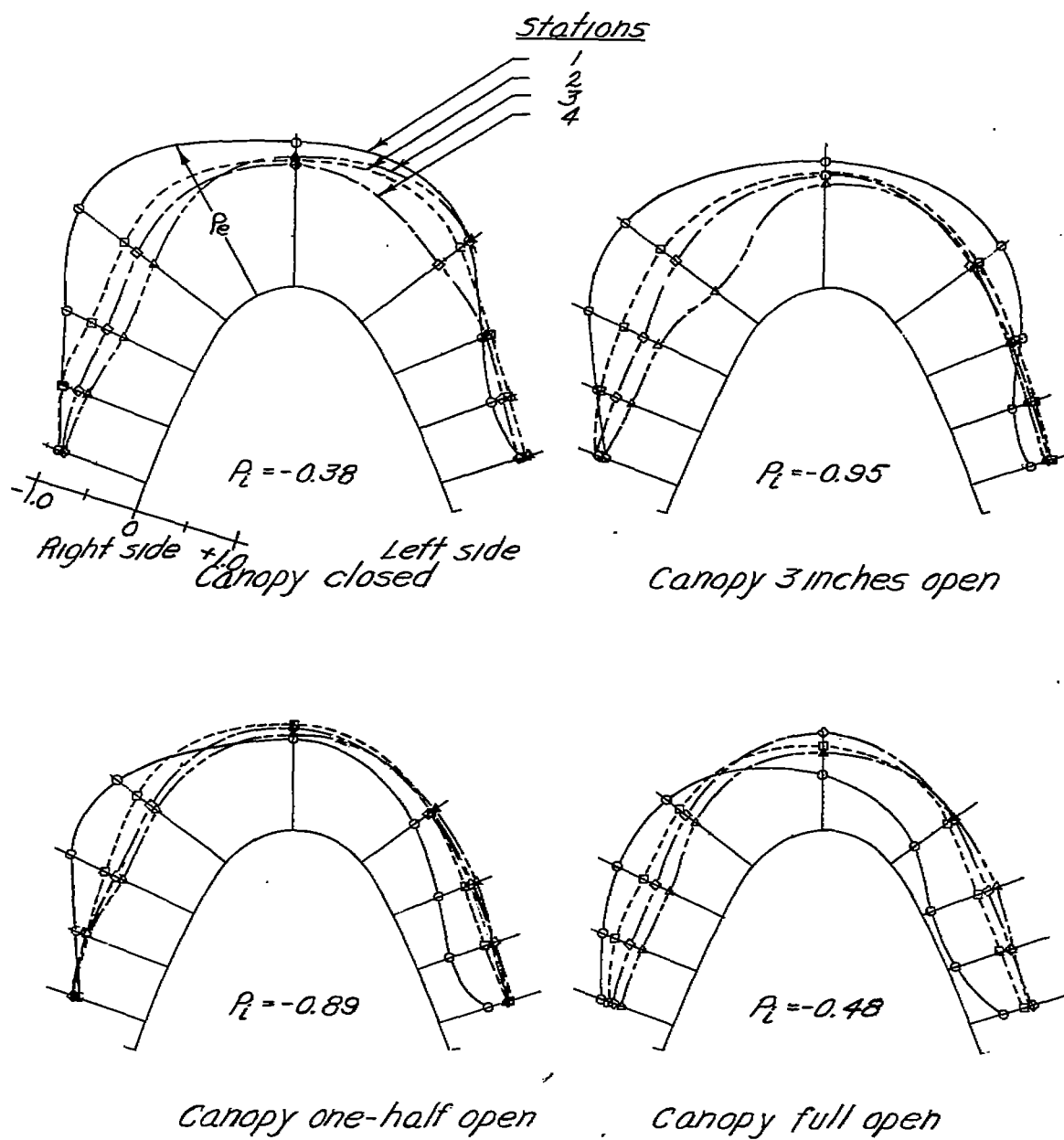
Figure 10.- continued.



NATIONAL ADVISORY  
COMMITTEE FOR AERONAUTICS

(c) Military power;  $T_c, 0.36$ ;  $C_L, 0.91$

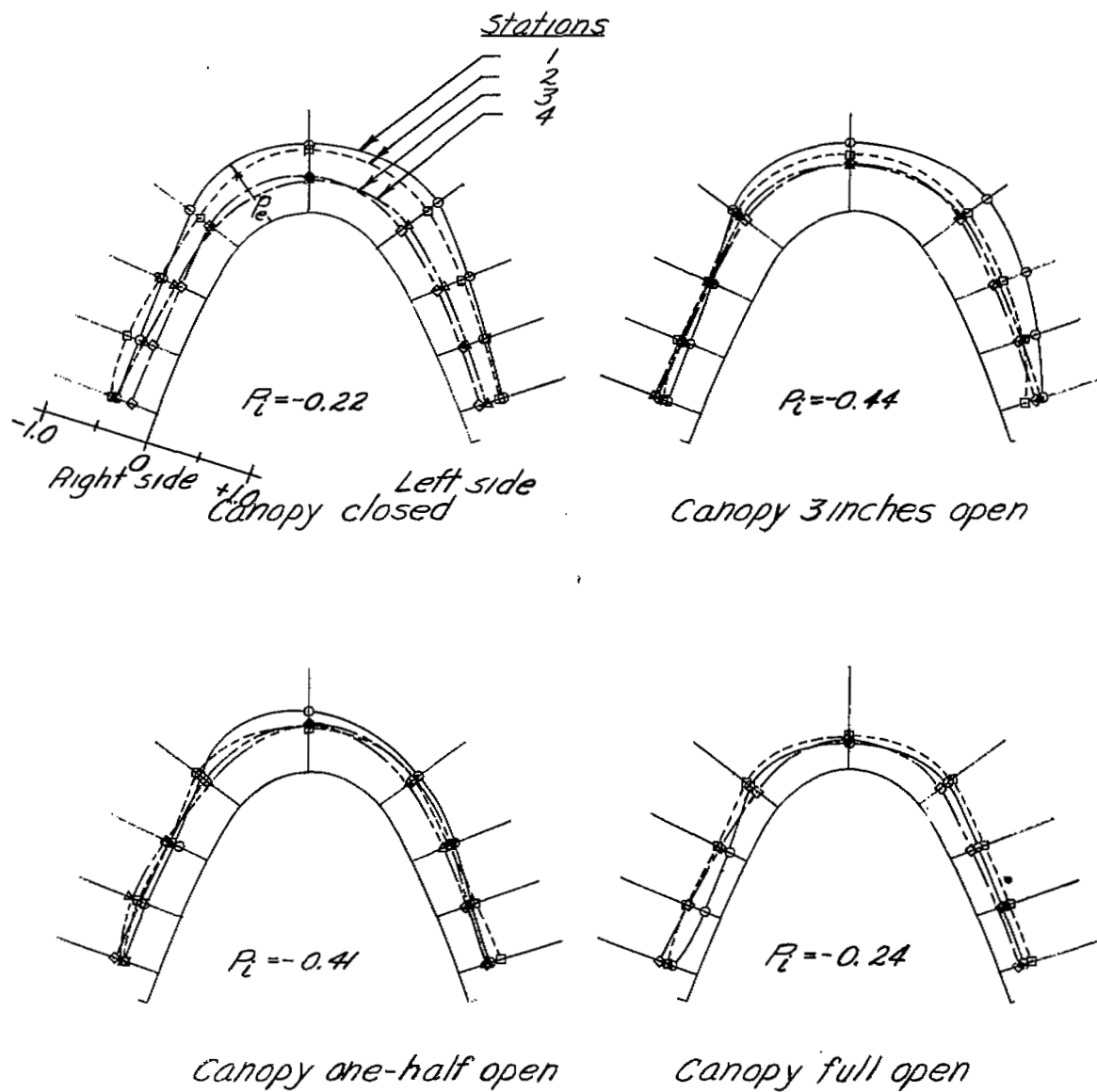
Figure 10.- continued.



NATIONAL ADVISORY  
COMMITTEE FOR AERONAUTICS

(d) Military power;  $T_c, 0.53$ ;  $C_L, 1.23$

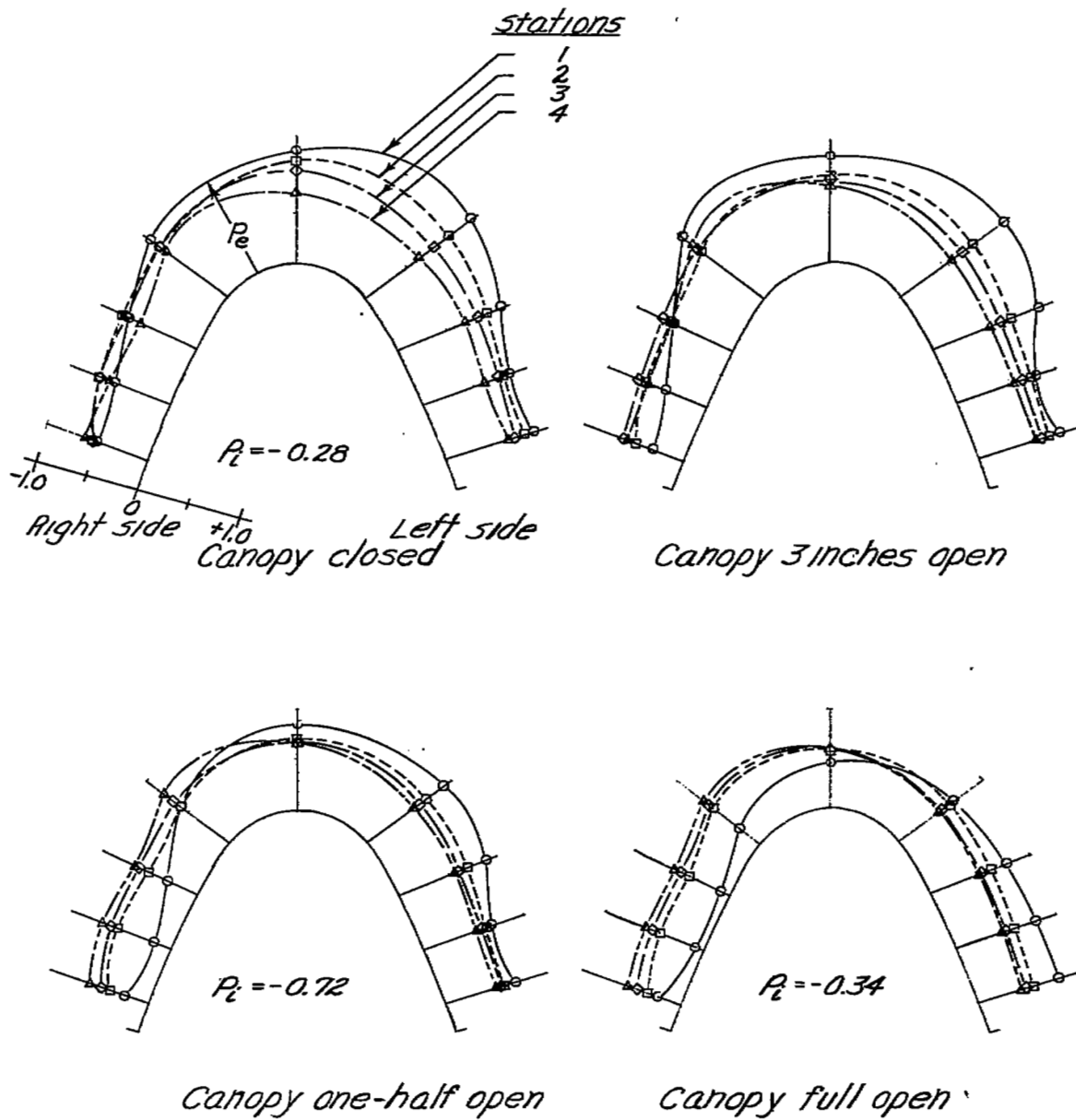
Figure 10.- continued.



NATIONAL ADVISORY  
COMMITTEE FOR AERONAUTICS

(e) Propeller idling;  $C_l, 1.23$

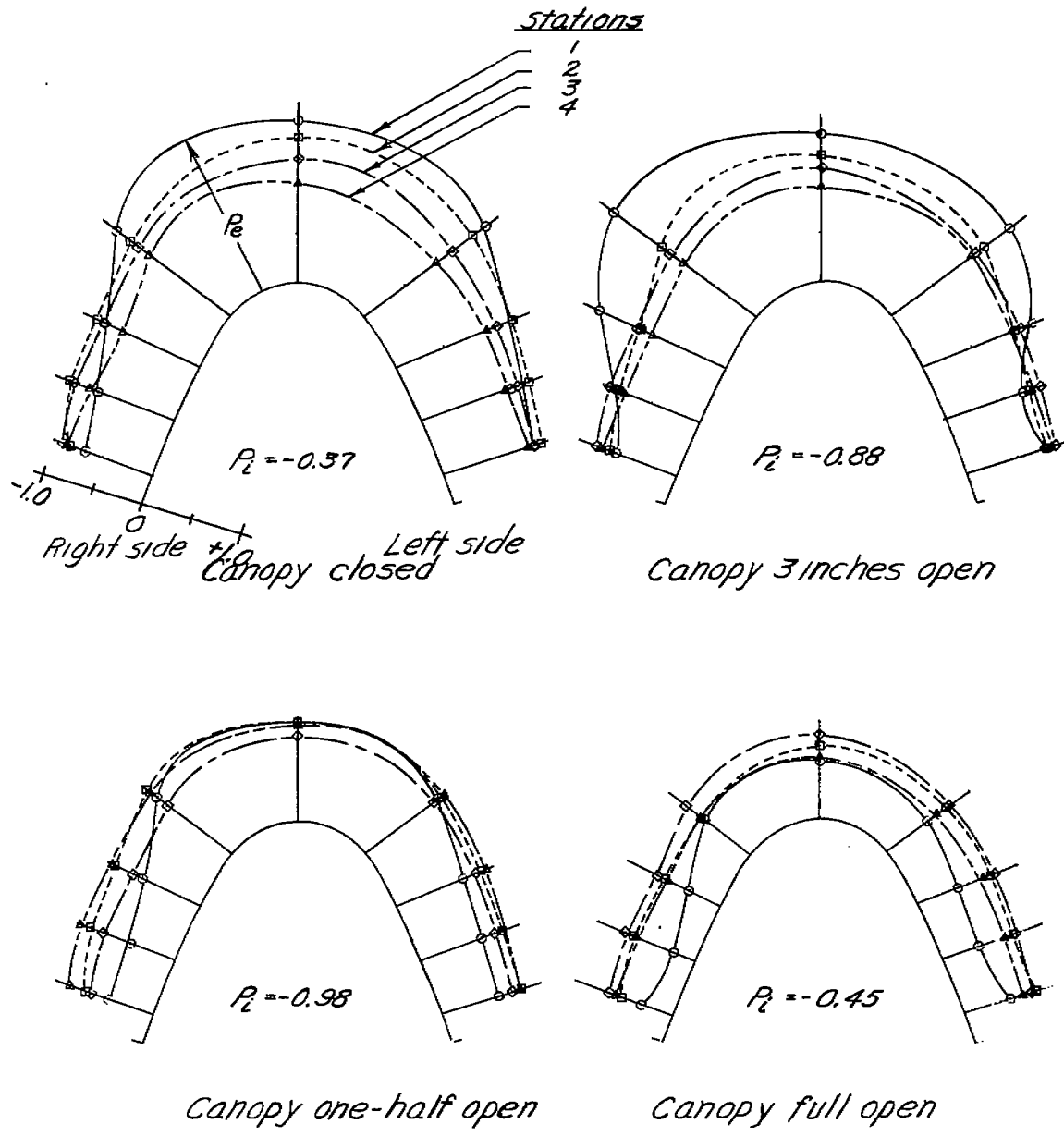
Figure 10. - concluded.



NATIONAL ADVISORY  
COMMITTEE FOR AERONAUTICS

(a) Military power;  $T_0, 0.36$ ;  $C_L, 0.91$

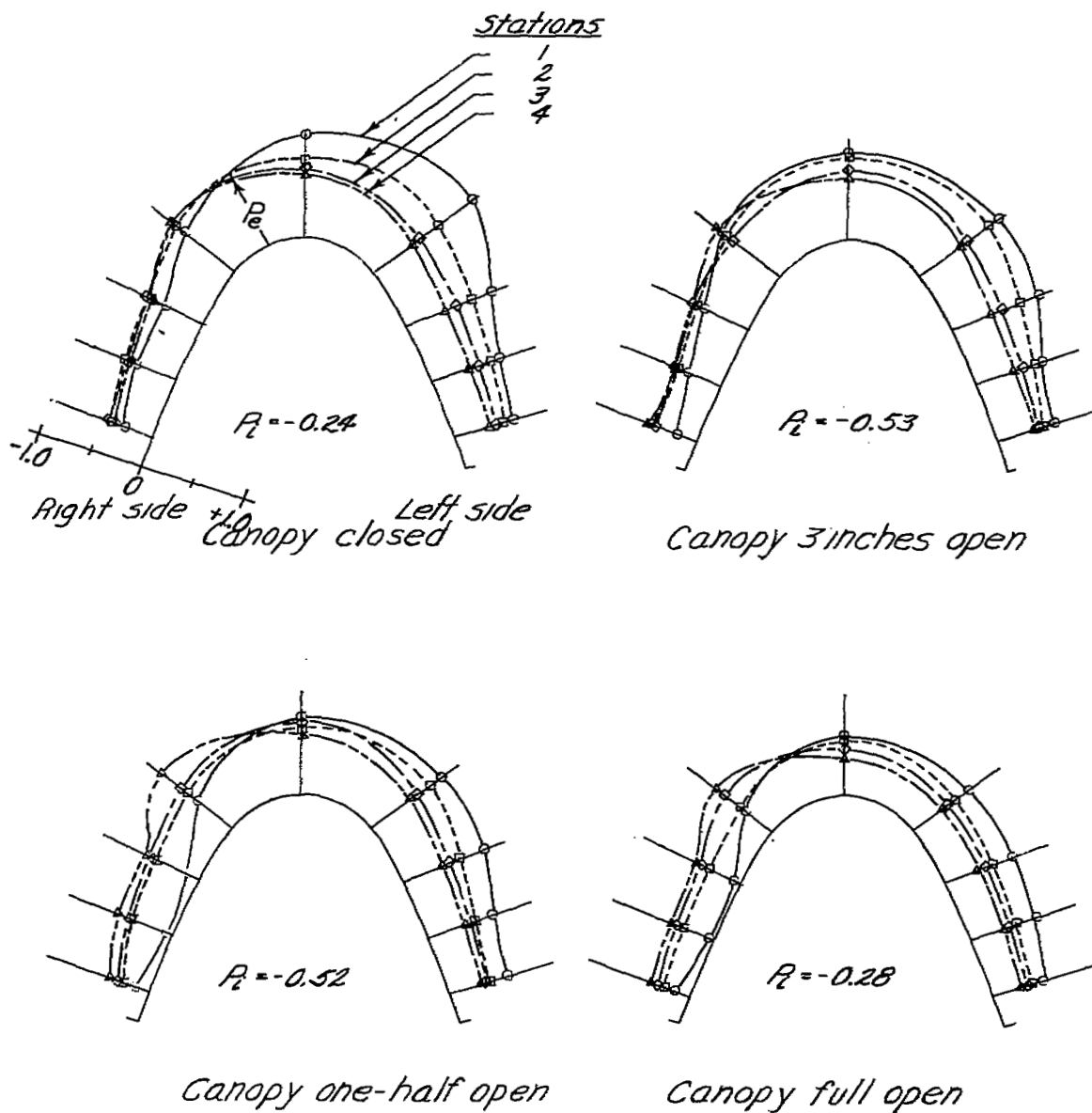
Figure 11 - Pressure distributions over the canopy of the F6F-3 airplane.  $\psi, 15^\circ$



NATIONAL ADVISORY  
COMMITTEE FOR AERONAUTICS

(b) Military power;  $T_c, 0.53$ ;  $C_L, 1.23$

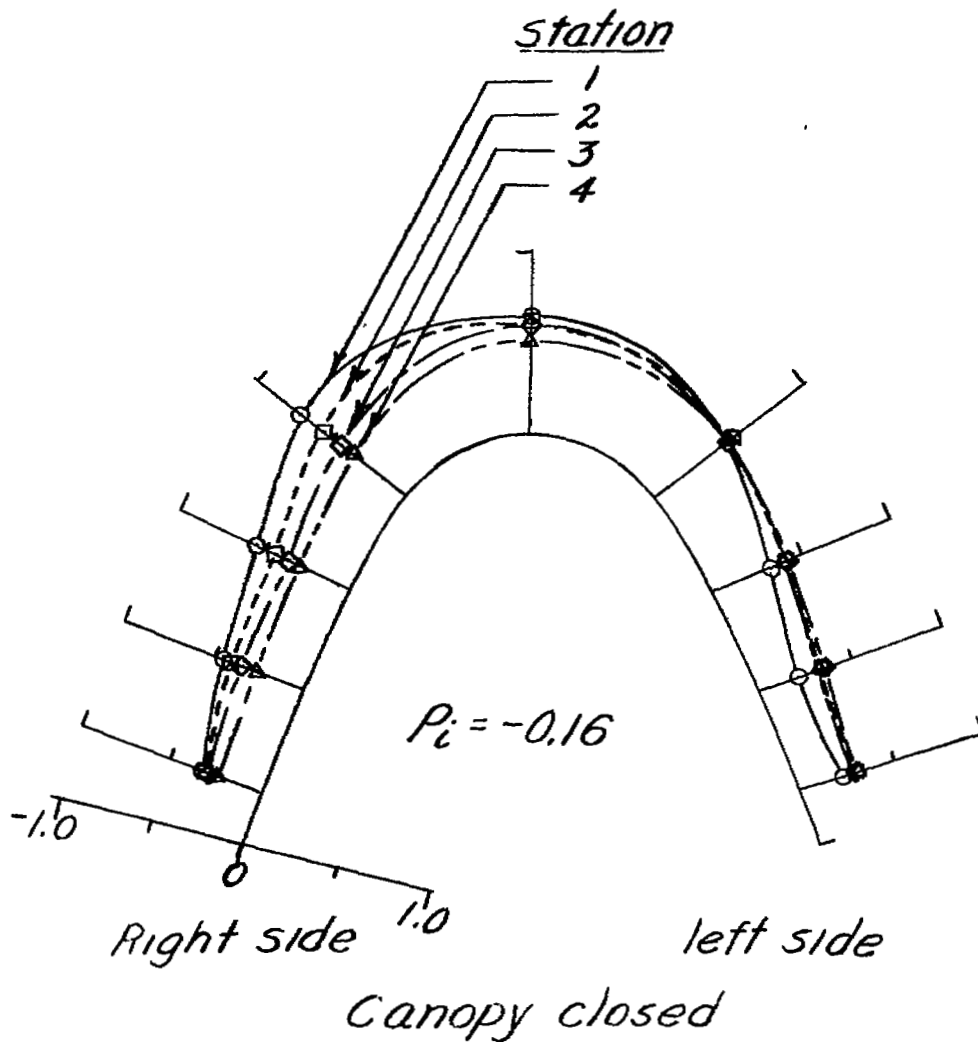
Figure 11.- continued.



NATIONAL ADVISORY  
COMMITTEE FOR AERONAUTICS

(c) Propeller idling;  $C_L, 1.23$

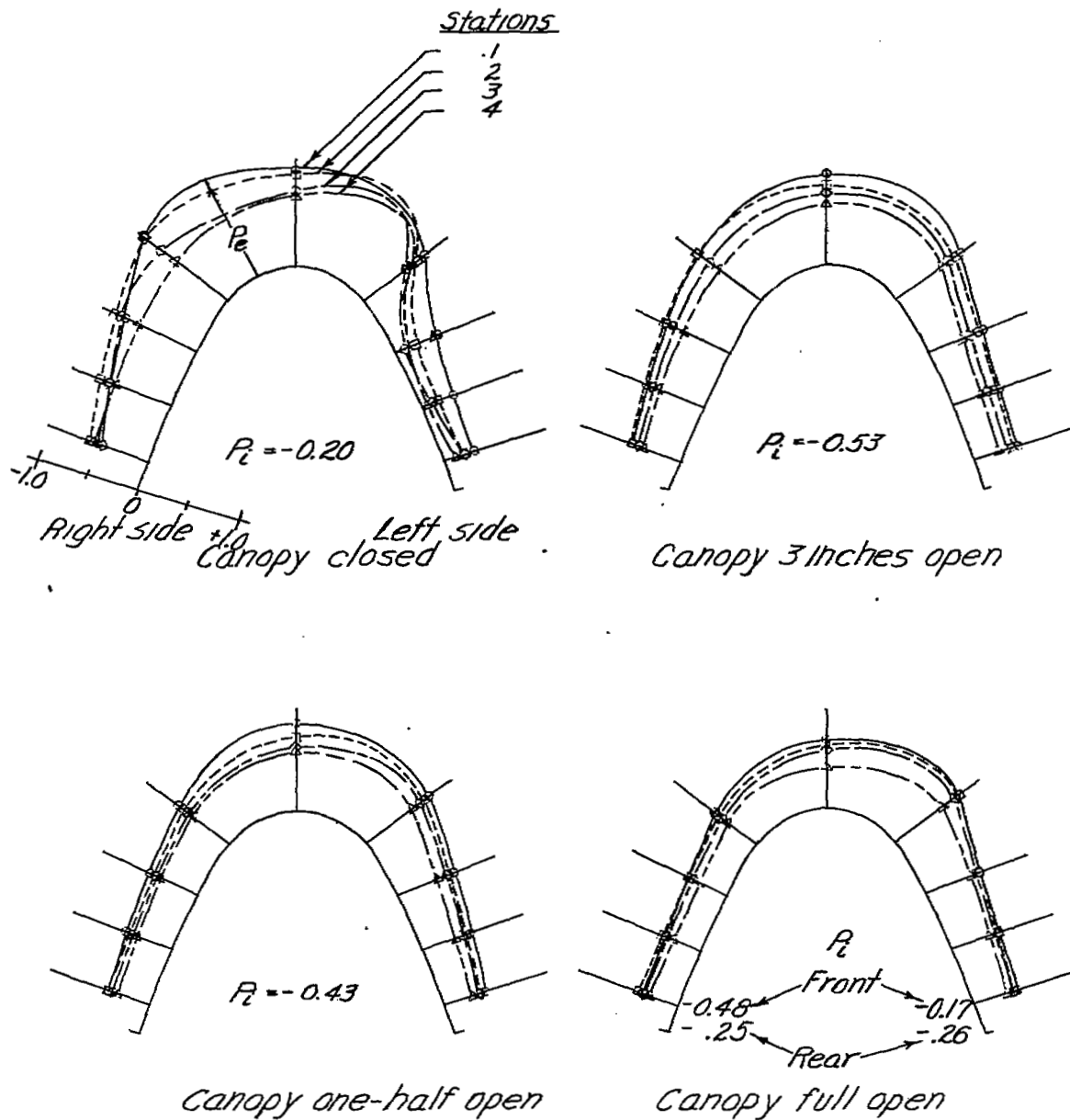
Figure 11. -, concluded.



(a) Military power;  $T_c, 0.04$ ;  $C_L, 0.20$

NATIONAL ADVISORY  
COMMITTEE FOR AERONAUTICS

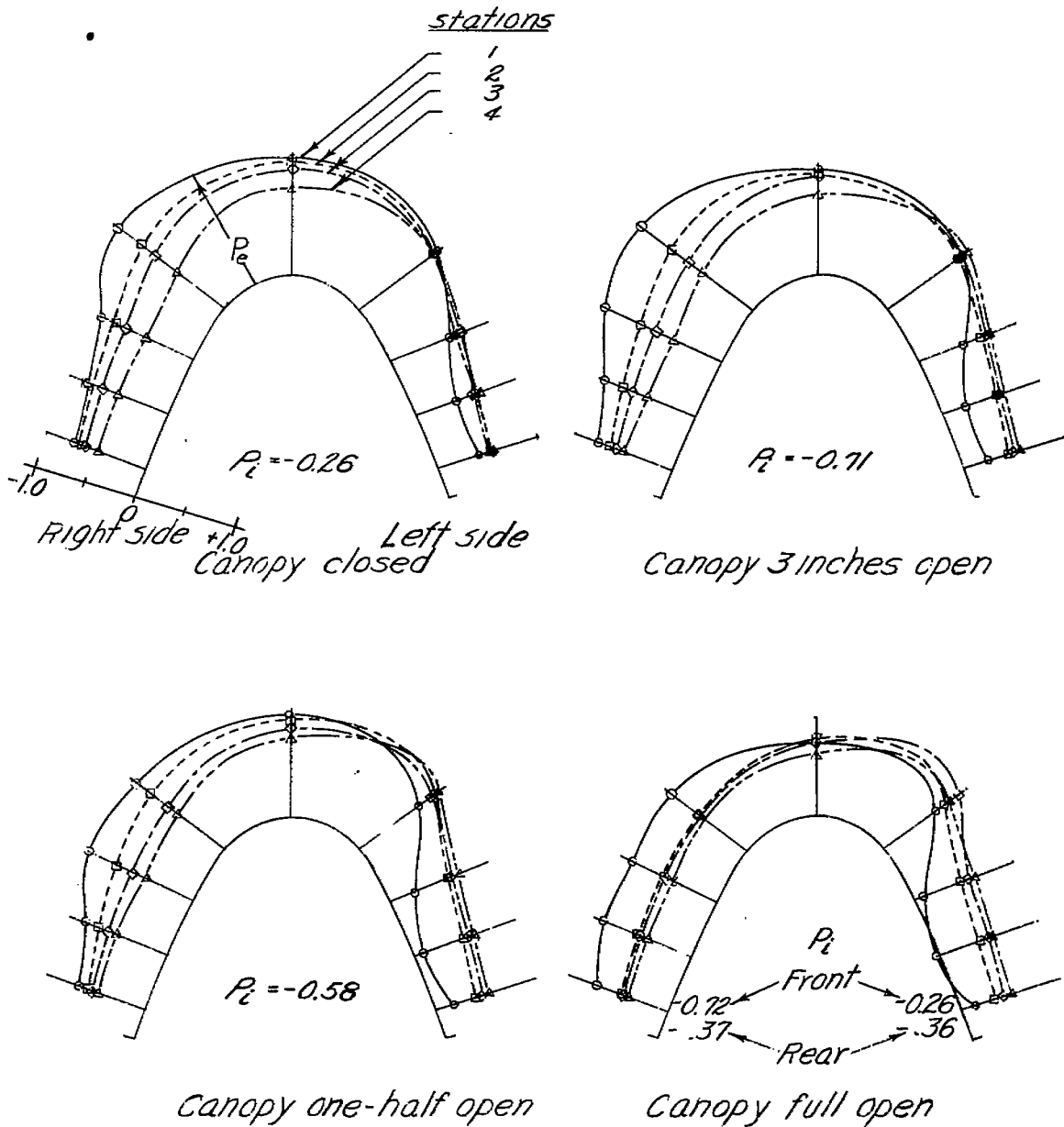
Figure 12.- Pressure distributions over the canopy of the F6F-3 airplane.  $\psi, 7.5^\circ$



NATIONAL ADVISORY  
COMMITTEE FOR AERONAUTICS

(b) Military power;  $T_c, 0.18$ ;  $C_L, 0.52$

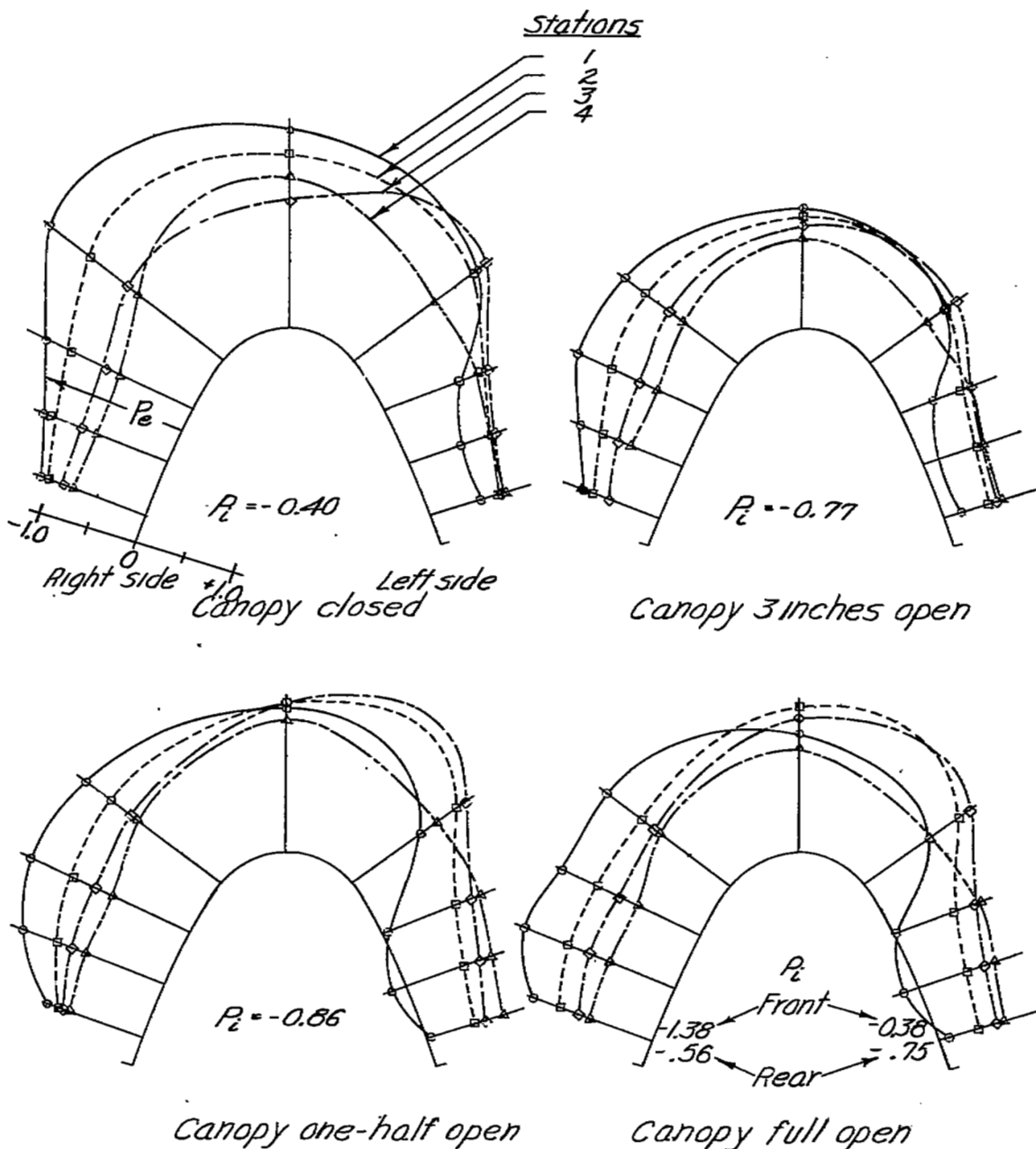
Figure 12.- continued.



NATIONAL ADVISORY  
COMMITTEE FOR AERONAUTICS

(c) Military power;  $T_c, 0.36$ ;  $C_L, 0.91$

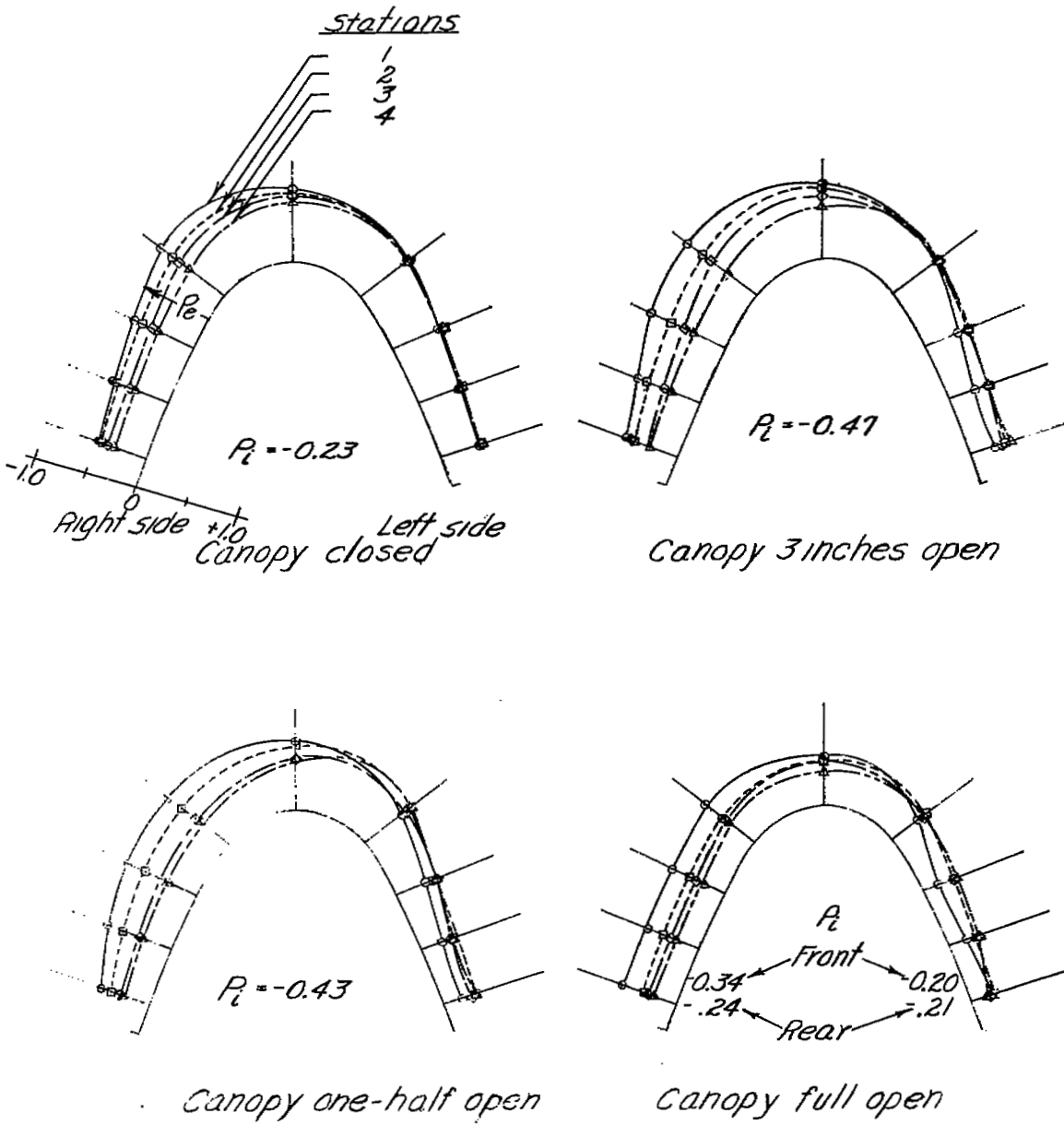
Figure 12.- continued.



NATIONAL ADVISORY  
COMMITTEE FOR AERONAUTICS

(d) Military power;  $T_c, 0.53$ ;  $C_L, 1.23$

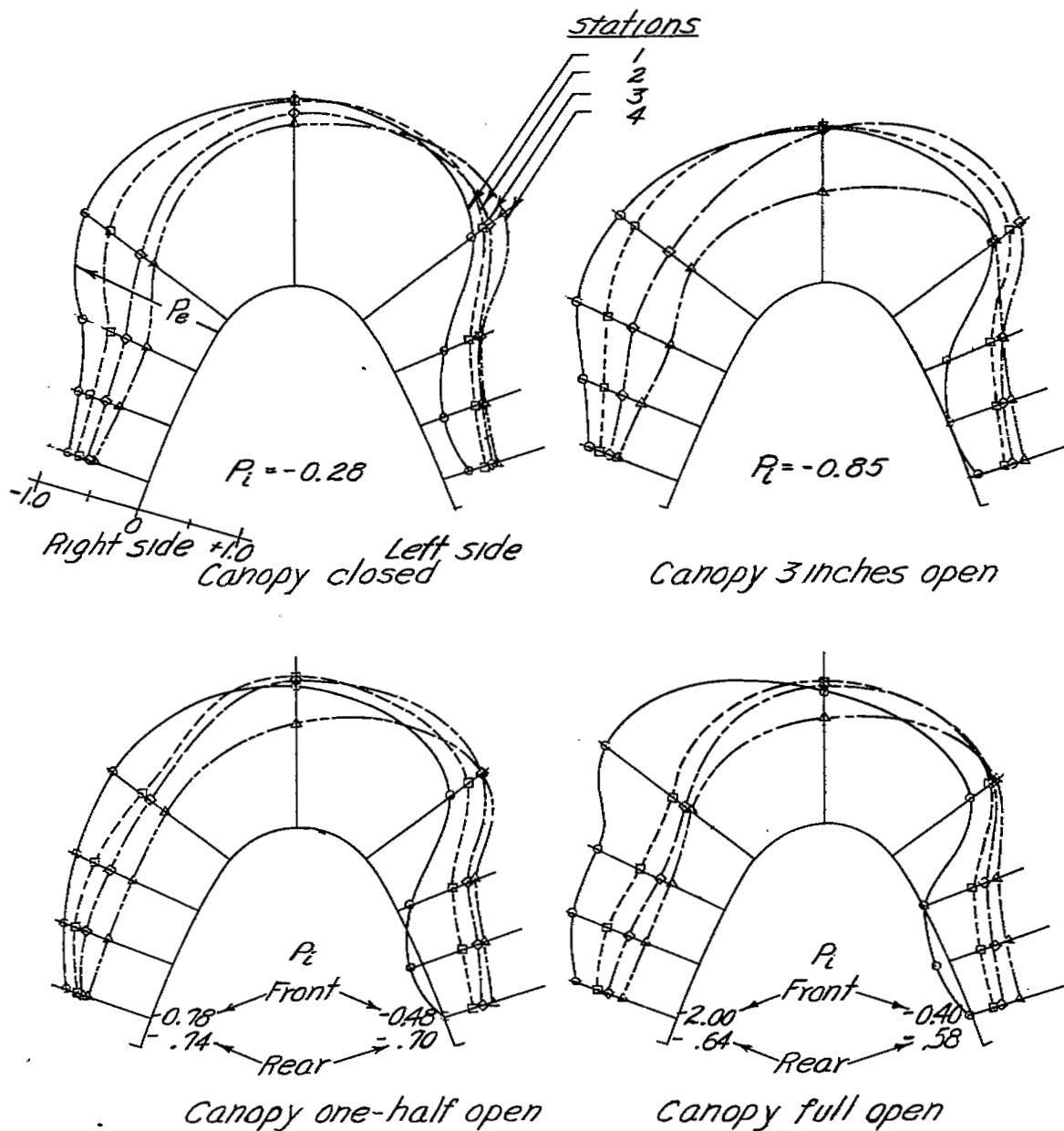
Figure 12. - continued.



NATIONAL ADVISORY  
COMMITTEE FOR AERONAUTICS

(e) Propeller idling;  $C_L, 1.23$

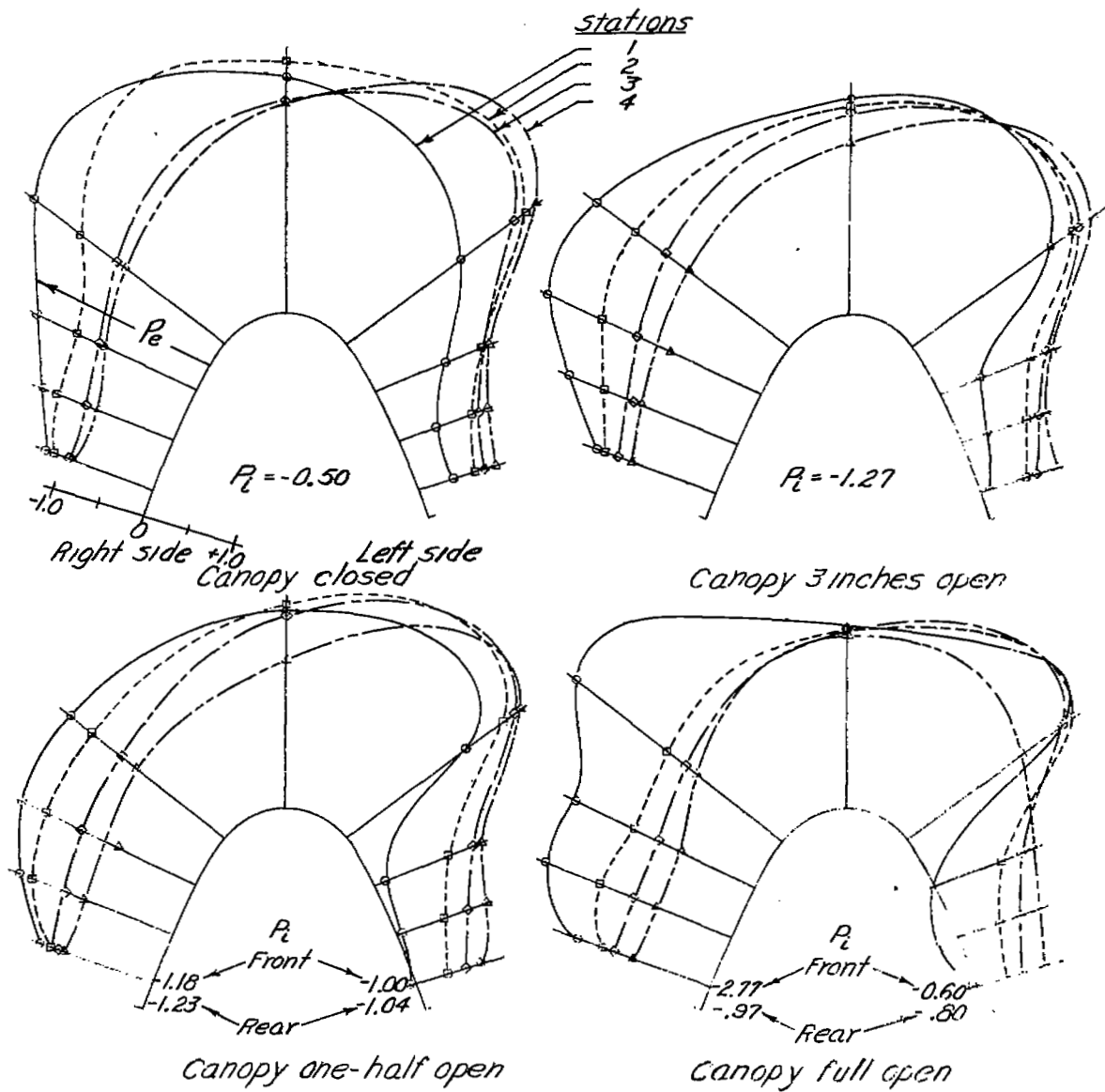
Figure 12.- concluded.



NATIONAL ADVISORY  
COMMITTEE FOR AERONAUTICS

(a) Military power;  $T_c, 0.36$ ;  $C_L, 0.91$

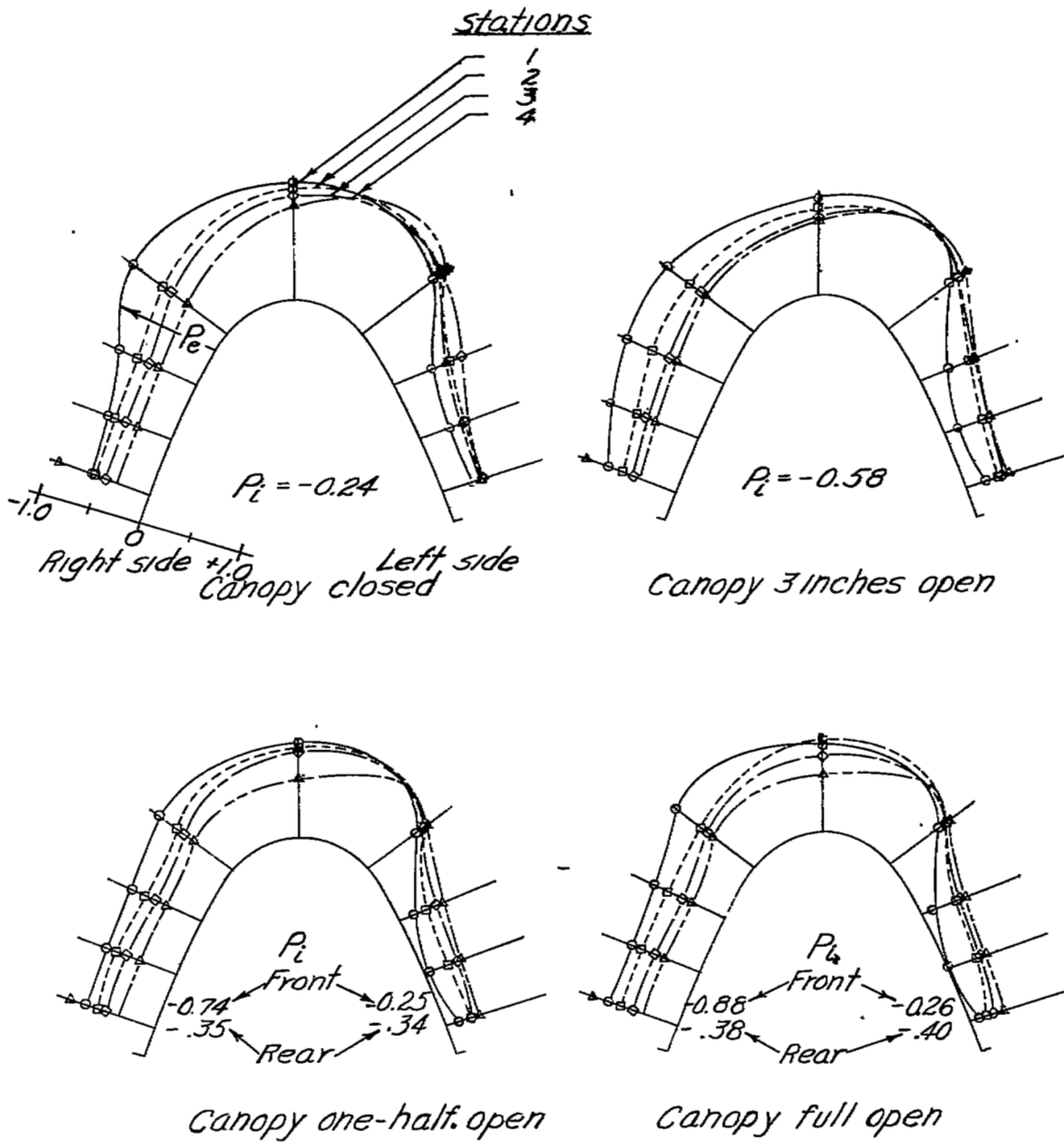
Figure 13 - Pressure distributions over the canopy of the F6F-3 airplane.  $\psi, 15^\circ$



NATIONAL ADVISORY  
COMMITTEE FOR AERONAUTICS

(b) Military power;  $T_c, 0.53$ ;  $C_L, 1.23$

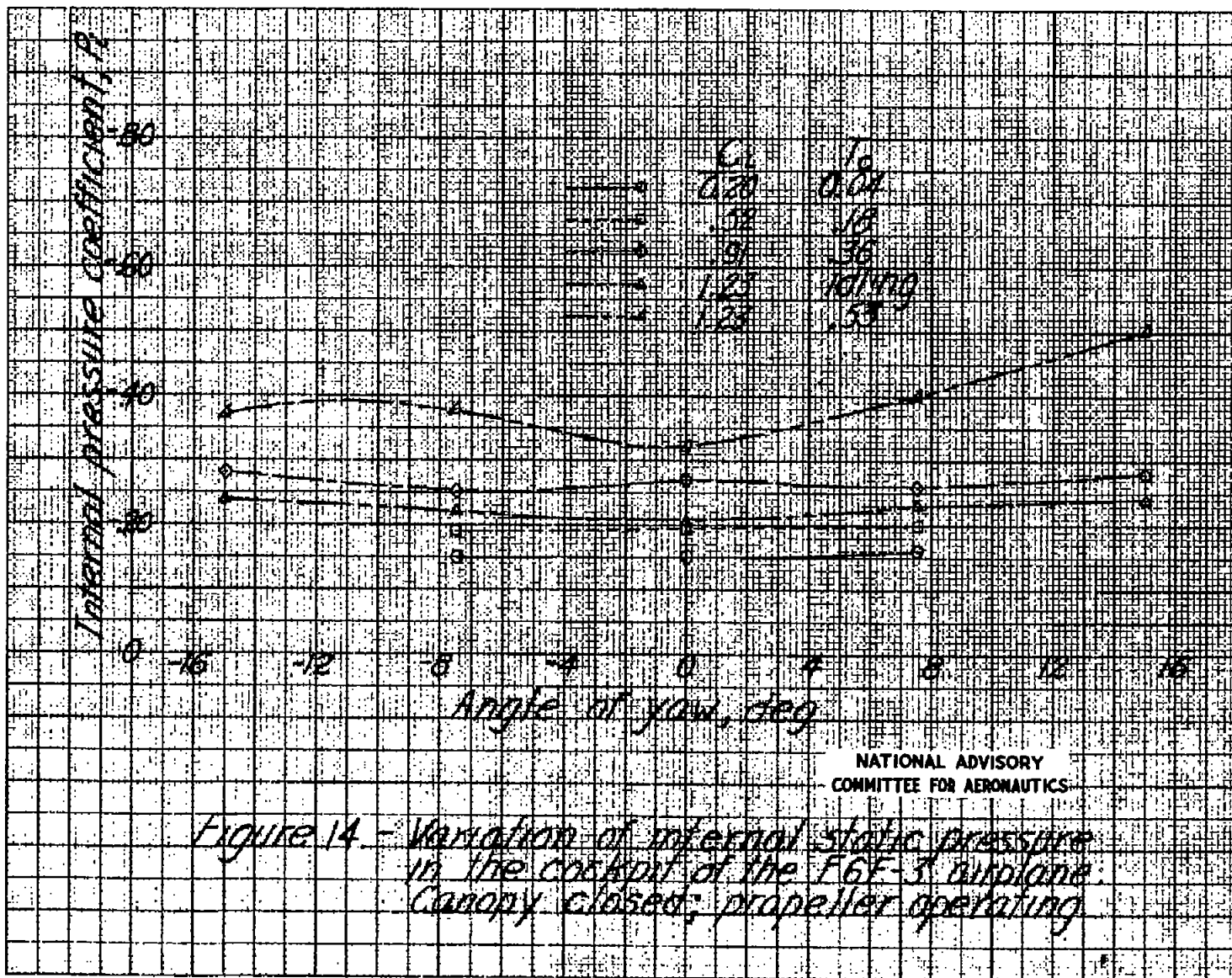
Figure 13.- continued.



NATIONAL ADVISORY  
COMMITTEE FOR AERONAUTICS

(c) Propeller idling;  $C_L, 1.23$

Figure 13.-concluded.



NASA Technical Library



3 1176 01437 0309